OPEN ACCESS

Repository of the Max Delbrück Center for Molecular Medicine (MDC) in the Helmholtz Association

https://edoc.mdc-berlin.de/16777

NF-κB participates in mouse hair cycle control and plays distinct roles in the various pelage hair follicle types

Krieger K., Millar S.E., Mikuda N., Krahn I., Kloepper J.E., Bertolini M., Scheidereit C., Paus R., Schmidt-Ullrich R.

This is the final version of the accepted manuscript. The original article has been published in final edited form in:

Journal of Investigative Dermatology
2018 FEB ; 138(2): 256-264
2017 SEP 20 (first published online: final publication)
doi: 10.1016/j.jid.2017.08.042

Publisher: Elsevier

Erratum in: Journal of Investigative Dermatology 138(9): 2084
https://doi.org/10.1016/j.jid.2018.06.173

Copyright © 2017 The Authors. Published by Elsevier, Inc. on behalf of the Society for Investigative Dermatology. This manuscript version is made available under the Creative Commons Attribution-NonCommercial-NoDerivatives 4.0 International License. To view a copy of this license, visit http://creativecommons.org/licenses/by-nc-nd/4.0/ or send a letter to Creative Commons, PO Box 1866, Mountain View, CA 94042, USA.

NF-κB participates in mouse hair cycle control and plays distinct roles in the various pelage hair follicle types

Karsten Krieger[1], Sarah E. Millar[2], Nadine Mikuda[1], Inge Krahn[1], Jennifer E. Kloepper[3], Marta Bertolini[5], Claus Scheidereit[1], Ralf Paus[4], Ruth Schmidt-Ullrich[1*]

[1] Signal Transduction in Tumor Cells, Max-Delbrück-Center (MDC) for Molecular Medicine, Berlin, Germany.

[2] Departments of Dermatology and Cell and Developmental Biology, Perelman School of Medicine, University of Pennsylvania, Philadelphia, PA, USA

[3] Department of Dermatology, University of Lübeck, Lübeck, Germany.

[4] Department of Dermatology, University of Münster, Münster, Germany & Centre for Dermatology Research, University of Manchester, Manchester, UK

[5] Department of Dermatology, University of Münster, Münster, Germany

* Corresponding author: Ruth Schmidt-Ullrich: Tel. +49-30-9406 3756, FAX +49-30-9406 3884, e. mail rschmidt@mdc-berlin.de.

Short title: NF-κB in the hair cycle

ABSTRACT

The transcription factor NF-κB controls key features of hair follicle (HF) development, but the role of NF-κB in adult HF cycle regulation remains obscure. Using NF-κB reporter mouse models, strong NF-κB activity was detected in the secondary hair germ (SHG) of late telogen and early anagen HFs, suggesting a potential role for NF-κB in HF stem/progenitor cell activation during anagen induction. At mid-anagen, NF-κB activity was observed in the inner root sheath (IRS) and unilaterally clustered in the HF matrix, which indicates that NF-κB activity is also involved in hair fiber morphogenesis during HF cycling. A mouse model with inducible NF-κB suppression in the epithelium revealed pelage hair-type-dependent functions of NF-κB in cycling HFs. NF-κB participates in telogen-anagen transition in awl and zigzag HFs, and is required for zigzag hair bending and guard HF cycling. Interestingly, zigzag hair shaft bending depends on non-canonical NF-κB signaling, which previously has only been associated with lymphoid cell biology. Furthermore, loss of guard HF cycling suggests that in this particular hair type NF-κB is indispensable for stem cell activation, maintenance and/or growth.

INTRODUCTION

The hair follicle (HF) undergoes lifelong tissue remodeling cycles which involve intensive molecular interactions between the epithelial and mesenchymal part of the HF, and between the HF and its macroenvironment (Plikus and Chuong, 2014, Schneider et al., 2009). Molecular regulators of the hair cycle include WNT, SHH, TGF-β2, FGFs and BMP signals, all of which also play important roles in HF development (Choi et al., 2013, Hsu et al., 2014, Oshimori and Fuchs, 2012, Plikus et al., 2008, Schneider et al., 2009).

In HF development, NF-κB activity is required for primary guard HF formation and zigzag hair fiber morphogenesis downstream of the TNF family member EDA-A1 and its receptor EDAR (Schmidt-Ullrich et al., 2006). EDA-A1 and EDAR proteins are also expressed in adult cycling pelage HFs, suggesting possible functions for EDA-A1/EDAR signaling in the hair cycle (Elomaa et al., 2001, Fessing et al., 2006). Furthermore, during hair follicle development NF-κB orchestrates WNT, BMP and SHH signaling, all of which also play important roles in the hair cycle (Bazzi et al., 2007, Fliniaux et al., 2008, Mou et al., 2006, Pummila et al., 2007, Schmidt-Ullrich et al., 2006, Tomann et al., 2016, Zhang et al., 2009). Recently, extensive NF-κB target gene analyses revealed that NF-κB controls the expression of transcription factors *Sox9* and *Lhx2* (Tomann et al., 2016) which regulate HF stem cell (HFSC) maintenance and activation (Folgueras et al., 2013, Kadaja et al., 2014, Rhee et al., 2006, Vidal et al., 2005). Together, these observations strongly suggest a role for NF-κB in the hair cycle. However, the precise functions and regulation of NF-κB in the hair cycle remain obscure.

To address this question, HF cycle-associated NF-κB activity was examined using NF-κB reporter mice (Tomann et al., 2016), which revealed activity in key regulating sites. To analyze NF-κB functions in the hair cycle of all pelage HF types, independent of morphogenetic defects,

we generated mice with doxycycline-inducible NF-κB suppression in the epithelium. We show that NF-κB promotes anagen induction and growth of awl and zigzag follicles and is required for guard HF cycling. Moreover, we verify a requirement for non-canonical NF-κB signaling in hair shaft bending.

RESULTS

NF-κB activity is detected in the SHG, IRS and anagen hair bulb

To investigate NF-κB functions in the hair cycle, two NF-κB reporter mouse lines that use either β-galactosidase activity *(κ-Gal*; Figure 1a) or EGFP (*κ-EGFP*; Figure 1a-b, Supplementary Figure S1 online) as read-out for NF-κB activity were analyzed for reporter gene expression at successive hair cycle phases (Schmidt-Ullrich et al., 1996, Tomann et al., 2016).

At the second postnatal telogen phase (P53), strong 4-chloro-5-bromo-3-indoyl β-D-galactopyranoside (X-Gal) staining for β-galactosidase and EGFP expression were observed in the secondary hair germ (SHG), the lower bulge, and around the sebaceous gland (SG) (Figure 1a). In early anagen follicles, one to three days after back skin depilation to induce anagen, NF-κB activity was observed in the SHG (d1, d3; Figure 1b). At mid-anagen, five days after depilation (d5), most activity co-localized with nuclear phospho-p65 in a unilateral cluster of HF matrix cells (Figure 1b, d), and in the inner root sheath (IRS) (Figure 1b). The distinctive NF-κB activity in the SHG and lower bulge suggested a role for NF-κB-mediated signaling in HFSC activation during anagen induction and/or progenitor cell proliferation to form the anagen HF matrix. Note that NF-κB activity was observed in the SHG, the SG area, IRS and the hair bulb of anagen follicles following depilation as well as in the absence of depilation (Figure 1a-b, Supplementary Figure S1). Furthermore, we did not detect any increased apoptosis in *K5-ΔN* mice when compared to controls at d1 – d5 (data not shown). This demonstrates that in our experimental settings NF-κB activity in anagen HFs is independent of inflammatory and cell death signals which may be caused by depilation (Chen et al., 2015, Ito et al., 2002).

At d16, when hair follicles begin to enter catagen, some residual NF-κB activity was observed in the IRS (Figure 1d). In telogen HFs (d21) NF-κB activity was again detected in the SGH (Figure 1d). mRNA expression of the *bona fide* NF-κB target gene *Nfkbia* (IκBα) at postnatal days P25 (anagen I) to P30 (full anagen) confirmed NF-κB activity in the SHG, IRS and unilaterally in the matrix (Supplementary Figure S2). As expected, *Nfkbia* expression was absent in *ΔN* and *Edar*-mutant mice (*downless, dl*; Supplementary Figure S2).

Unilateral NF-κB reporter expression in the matrix from d5 (anagen III/IV) onwards was reminiscent of the expression of known regulators of hair shaft bending (Hammerschmidt and Schlake, 2007, Schlake, 2005, 2006), suggesting that NF-κB also controls bending in adult HFs (see below).

In early anagen HFs NF-κB activity co-localizes with expression of SHG markers

To further characterize HF cells with active NF-κB, expression of various markers for quiescent and activated HFSC, as well as for transit-amplifying cells (TAC) and other HF keratinocytes was analyzed in *κ-EGFP* mice (Figure 2 a-c). For this purpose co-expression of EGFP with transcription factors NFATc1, SOX9, LHX2 or TRPS1, or with Keratin 15 (K15), LGR5, SHH or EDAR was examined (Figure 2 a-c).

NF-κB activity was not observed in NFATc1-expressing quiescent bulge HFSC (Figure 2a). However, in activated bulge HFSC progenitors of the SHG NF-κB activity co-localized with K15 and LHX2 expression, and with some SOX9-expressing cells (Figure 2a; d3, early anagen). *Lhx2* and *Sox9* were identified as NF-κB target genes (Tomann et al., 2016), and both markers are essential for maintenance of HFSC and the stem cell niche (Folgueras et al., 2013, Nowak et al.,

2008). However their strong expression in the SHG suggests an additional role in anagen induction/HFSC activation (Tornqvist et al., 2010). Furthermore, expression of intestinal and cycling HF stem cell marker LGR5 (Barker et al., 2007, Jaks et al., 2008) co-localized with NF-κB activity in the SHG (Figure 2b). Strong NF-κB activity was also observed in TACs together with SHH and EDAR expression (Figure 2a). EGFP/EDAR co-expression was restricted to the TAC area, which suggests that in TACs, NF-κB activity may be regulated by EDA-A1/EDAR signaling (Figure 2a). In summary, these results indicate a potential novel role for NF-κB in HFSC activation and TAC proliferation during anagen induction (see Suppl. Discussion).

In mid anagen NF-κB activity co-localizes with hair shaft bending markers

At mid-anagen (d5), when NF-κB activity shifted mainly to the HF matrix (Figure 1b), EGFP expression no longer co-localized with K15 or SOX9 expression (Figure 2c). However, co-expression of EGFP with EDAR, LHX2 and SHH remained and was confined unilaterally to the matrix (Figure 2c). TRPS1, that is a potential target gene of NF-κB in guard HF induction (Tomann et al., 2016) and is expressed in proliferating and differentiating cells of the lower HF (Fantauzzo et al., 2008), was also partially co-expressed with EGFP unilaterally in the HF matrix (Figure 2c). A role for SHH in hair shaft bending was suggested previously (Hammerschmidt and Schlake, 2007), however, the function of LHX2 and TRPS1 in hair shaft bending remains unknown.

NF-κB participates in anagen induction

Based on the localization of NF-κB activity in cycling HFs, we next examined hair cycle induction and progression. As *ΔN* mice only develop an intermediate awl hair type (Schmidt-Ullrich et al., 2001), we generated *K5rtTA;tetO-Cre*;*loxPΔN* mice in which NF-κB activity can be conditionally suppressed in the epithelium including HFs by oral administration of doxycycline (dox) (Supplementary Material and Discussion, Figures S3a-d, S4a-b). *K5rtTA;tetO-Cre*;*loxPΔN* mice allow analyzing NF-κB functions in the hair cycle for all pelage hair types.

In dox-treated *K5rtTA;tetO-Cre*;*loxPΔN* mice (here *K5-ΔN*), the transition from telogen to anagen was delayed, as indicated by a reduced hair cycle score (HCS) and percentage of HFs that had entered anagen I when compared to untreated *K5rtTA;tetO-Cre*;*loxPΔN* mice (controls) (Figure 3a-b, Supplementary tables S1 and S2). At mid-anagen (d5) *K5-ΔN* HFs continued to exhibit a decreased HCS and percentage of HFs in anagen IIIb-IV when compared to controls (Figure 3a-b, Supplementary tables S1 and S2).

At d10, HFs of *K5-ΔN* and control mice were indistinguishable in terms of hair cycle stage, with equal HCS and percentage of anagen IV-VI HFs in *K5-ΔN* mice and controls (Figure 3a-b, Supplementary tables S1 and S2). This indicated that once anagen has developed, the HFs completed anagen normally.

Due to delayed anagen development, catagen entry (d16) and progression (d18) and telogen transition (d25) were again retarded in *K5-ΔN* mice when compared to controls (Figure 3a-b, Supplementary tables S1 and S2). This was supported by an overall reduced HCS and percentage of HFs in distinct catagen phases and in telogen (d25) for *K5-ΔN* mice compared to controls (Figure 3a-b, Supplementary tables S1 and S2).

These data suggest that NF-κB assists anagen induction (Figure 3c). However, the overall delay in hair cycle progression and completion in *K5-ΔN* mice is due to the delayed telogen-anagen transition (see Figure 3c). Note that *ΔN* mice showed a reduced HCS at d2 and d5 and delayed anagen induction in the absence of depilation comparable to dox-treated *K5-ΔN* mice (data not shown and Supplementary Figure S5). Importantly, *ΔN* mice only develop awl and zigzag follicles (Schmidt-Ullrich et al., 2001), which suggests that the hair cycle defects observed in *K5-ΔN* mice may particularly affect these two HF types.

Proliferation of HFSC progenitors and HF and fiber length partly depend on active NF-κB

In search of the reason for delayed anagen induction in *K5-ΔN* mice, we analyzed proliferation in anagen follicles, and HF and fiber length (Figure 4). At d1 (anagen I), immunoreactivity for proliferation marker Ki67 was decreased by 50% in the SHG of *K5-ΔN* mice when compared with controls (Figure 4a). This finding partly explains the delayed anagen development in *K5-ΔN* mice and suggests a direct or indirect role for NF-κB in HFSC progenitor proliferation.

However, at d10 Ki67 staining showed abundant expression in *K5-ΔN* and control hair bulbs (Figure 4b). Furthermore, neither BrdU incorporation nor TUNEL staining revealed any differences between *K5-ΔN* and controls at d10 (data not shown). These data suggest that once anagen has been initiated, NF-κB is no longer required for maintaining cell proliferation in the hair bulb.

Anagen progression is characterized by increasing HF and fiber length (Schneider et al., 2009). At d5, *K5-ΔN* mice showed a reduced HF length when compared with controls (Figure 4c), and at

d18, hair fiber length was decreased by 15%-20% in *K5-ΔN* mice when compared with controls (Figure 4d). Because of unaltered anagen progression (see above) the mechanism behind the reduced HF growth and fiber length in *K5-ΔN* mice remains unknown. Possible reasons may be reduced/delayed hair shaft production or altered hair matrix keratinocyte differentiation in *K5-ΔN* mice.

Non-canonical NF-κB signalling is required for hair shaft bending

In *ΔN* mice zigzag fibers lack their characteristic bending (Schmidt-Ullrich et al., 2001). A potential role for NF-κB in hair shaft bending during the hair cycle was thus investigated and revealed ≥ 90% straight awl-type hair fibers in *K5-ΔN* mice at d10 (Figures 5a, 6c). Quantification of hairs at d18, d21 and d25 showed strongly reduced numbers of zigzag hairs and a proportional increase in awl-type hairs (Figure 5b).

Hair shaft bending appears to be regulated by asymmetric proliferation rates in the bulb (Schlake, 2007). In line with this, mRNAs of *Eda-A1*, of zigzag HF marker *Krox20* and of NF-κB targets *Nfkbia*, *Shh*, *Wnt10a*, *Wnt10b* and *Dkk4*, as well as of *ctnnb1* and *Ccnd1* were expressed unilaterally in hair bulbs of controls at P30 or d10, but were absent in *K5-ΔN* HFs (Figure 5c, Supplementary Figure S6a-b). However, in accordance with maintained zigzag follicle density in *K5-ΔN* and *ΔN* mice, expression of zigzag marker *Igfbp5* remained unaltered (Figure 5c, Supplementary Figure S6a). It has previously been suggested that hair shaft bending is regulated by WNT, EDA-A1 and downstream SHH signaling (Hammerschmidt and Schlake, 2007). Our data indicate that in the HF cycle EDA-A1 signaling also controls NF-κB activity to generate hair shaft bending. While overall WNT activity in the hair bulb of *K5-ΔN* mice was unaltered compared to controls, unilateral WNT activity and *Wnt* expression were absent (Figure 5c,

Supplementary Figure S6a and S7), suggesting that EDA-A1/EDAR/NF-κB controls SHH and WNT signaling in hair shaft bending.

Lack of zigzag hairs in Lymphotoxin-β (LT- β) KO mice suggested a possible involvement of non-canonical NF-κB signaling (Cui et al., 2006). Canonical NF-κB signaling regulates expression of non-canonical NF-κB subunits RelB and p100/p52, and of LT-β (Mordmuller et al., 2003, Sun, 2012, Yilmaz et al., 2014). To examine whether zigzag hair formation in *K5-ΔN* mice also depends on non-canonical signaling, protein and/or mRNA expression of RelB and p100 (*Nfkb2*) was analyzed in anagen HFs at d5 (Figure 5d, Supplementary Figure S8). RelB protein and *Nfkb2* and *RelB* mRNAs displayed unilateral expression in controls, but were absent in *K5-ΔN* mice (Figure 5d, Supplementary Figure S8a). p105 mRNA (*Nfkb1*) and protein (NFKB1) expression was also detected unilaterally in the hair bulb of controls and was absent in *K5-ΔN* (Supplementary Figure S8b). In line with *K5-ΔN* mice, *Nfkb1* KO mice (*Nfkb1*$^{-/-}$) did not generate any zigzag hairs (Figure 5a; Supplementary Figure S8c).

To demonstrate a requirement of non-canonical NF-κB signaling in hair shaft bending, *RelB* was deleted in an inducible manner in epithelial and HF keratinocytes (*K5-RelB*$^{-/-}$; Supplementary Material). Macroscopic analysis revealed the formation of only straight guard and awl-type hairs in *K5-RelB*$^{-/-}$ mice (Figure 5e).

These data confirm a role for non-canonical NF-κB signaling in hair shaft bending during the hair cycle. Non-canonical NF-κB most likely is activated by LTβ (Cui et al., 2006) that is upregulated by canonical EDA-A1/EDAR/NF-κB.

NF-κB activity is essential for maintenance of guard HFs

ΔN mice do not develop primary guard HFs (Schmidt-Ullrich et al., 2001). Therefore we hypothesized that upon inducible suppression of epithelial NF-κB activity, guard HF cycling might also be affected. This hair type only represents 2 - 10% of all pelage hairs and there are no adequate molecular markers to distinguish guards from large awl HFs. We thus relied on counting plucked guard hair fibers and on morphological identification of guard HFs in histological sections at d5 (Chi et al., 2013, Sundberg et al., 2005). Compared with controls, a significant reduction of guard hair fibers was observed in depilated *K5-ΔN* mice and in *K5-ΔN* mice that were treated with dox for 6-7 months in the absence of depilation (Figure 6a and b). Unlike in *ΔN* mice, loss of guard and zigzag hairs in *K5-ΔN* mice was not 100% which indicates that Cre-dependent depletion of NF-κB activity in *K5-ΔN* epithelial keratinocytes is mosaic (Figure 5a and b).

To confirm reduced guard hair fiber numbers, follicle morphology was analyzed in back skin sections (Figure 6c). As expected, in most control sections very large HFs with two sebaceous glands were observed (Figure 6c). In contrast, in *K5-ΔN* mice the percentage of guard HFs was significantly lower (Figure 6c). This indicates that NF-κB is required for guard HF maintenance during the adult hair cycle, but the molecular and physiological mechanisms remain unknown and may differ from guard HF development. Interestingly, *K5-RelB*$^{-/-}$ and *Nfkb1* KO mice had normal numbers of guard hairs which suggests that only canonical NF-κB signaling is required for guard HF cycling (Figure 5e, Supplementary Figure S8c).

DISCUSSION

NF-κB plays an important role in HF development, but its role in mature HF biology has remained unknown. Here we show that NF-κB is strongly activated in the SHG, IRS and in the hair bulb and provide evidence for involvement of NF-κB signaling in anagen induction. This role appears to be confined to awl and zigzag HFs, which are the only follicle types formed in *ΔN* (Schmidt-Ullrich et al., 2001) and *K5-ΔN* mice. Hair cycle-associated NF-κB activity is also required for hair shaft bending and for guard HF maintenance, which recapitulates NF-κB functions in embryonic HF development (Schmidt-Ullrich et al., 2001). This supports an important previous hypothesis that many signaling pathways which play a role in embryonic HF morphogenesis, including NF-κB, regulate analogous processes in anagen development and hair cycle progression (Schneider et al., 2009). In agreement with this, the SHG is often termed "placode" of the adult follicle, with both structures revealing strong WNT (Myung et al., 2013, Reddy et al., 2001) and NF-κB activity.

The mechanism behind the loss of guard HFs in *K5-ΔN* mice remains obscure. In early HF development NF-κB regulates signals (WNT, BMP inhibitors, SHH) that prevent premature placode keratinocyte differentiation and promote placode growth (Mou et al., 2006, Tomannet al., 2016). Thus, NF-κB activity in the SHG might prevent premature differentiation of the HFSC progeny and promote SHG cell proliferation. A significant reduction in Ki67-positive cells in the SHGs of *K5-ΔN* mice supports this hypothesis. This putative NF-κB function might be required particularly for guard HFs, which fail to undergo anagen development following depilation in *K5-ΔN* mice. Furthermore, the recently identified NF-κB/LHX2/TGFβ2 signaling axis may not only promote placode down-growth (Tomann et al., 2016), but also SGH proliferation and

growth. By contrast, no long-term loss of awl and zigzag follicles was observed in *K5-ΔN* mice (Figure 6b), suggesting that other signaling factors are able to compensate for the lack of NF-κB activity in the SHG of these HF types. Interestingly, unique lack of murine primary guard and human scalp HFs upon loss of EDA-A1/EDAR/NF-κB signaling (Doffinger et al., 2001, Monreal et al., 1999, Schmidt-Ullrich et al., 2001, Smahi et al., 2002) suggests analogies between these two follicle types regarding their molecular regulation and possibly their evolutionary origin. In human mid-anagen HFs NF-κB activity is required for anagen maintenance and, similarly to murine HFs, for hair fiber elongation (Kloepper et al., 2014).

We show here that non-canonical NF-κB signaling is a key regulator of hair shaft bending since zigzag hair formation is selectively lost when non-canonical signaling is blocked in the epithelium. Nevertheless, *ΔN*, *K5-ΔN*, *Nfkb1* KO and *K5-RelB*$^{-/-}$ mice share the same phenotype in terms of hair bending, because canonical NF-κB signaling is required to activate non-canonical signaling (Mordmuller et al., 2003). Interestingly, loss of zigzag hairs was also observed in mice that overexpress BMP antagonist Noggin (Sharov et al., 2006). This loss was due to an increased hair follicle size which indicates that BMP regulates hair bulb cell numbers (Sharov et al., 2006). In contrast, *K5-ΔN* and *ΔN* mice have mostly small-sized hair bulbs which would point to an increased number of zigzag hairs. We and others show that canonical/non-canonical NF-κB rather specifies hair fiber shape by regulating hair shaft axial polarity and asymmetric matrix cell proliferation downstream of EDA-A1 and LTβ signaling (Cui et al., 2006, Hammerschmidt and Schlake, 2007). Thus, hair fiber shape appears to be determined by hair bulb size, DP cell numbers and by axial polarity of the hair shaft and asymmetric proliferation in the hair matrix (Chi et al., 2013, Hammerschmidt and Schlake, 2007, Sharov et al., 2006). Finally, asymmetric matrix proliferation and a similar mRNA expression pattern of known NF-κB target genes,

including *Nfkbia*, *Wnt10a* and *10b*, *Shh*, *Dkk4*, and *Edar* in human (Kloepper et al., 2014) and murine mid-anagen HF bulbs suggest related mechanisms behind human curly and murine zigzag hair formation (see also (Schlake, 2007, Thibaut et al., 2005)).

This study supports a role for NF-κB in the murine hair cycle, and at the same time leaves a number of very interesting unanswered questions to be addressed in the future. These include the role of EDA/EDAR signaling in NF-κB regulation during the hair cycle and in TACs, the functions of the NF-κB/LHX2/TGFβ2 signaling axis in HF growth, and a role for NF-κB in human curly hair. Importantly, on the basis of our previous observation that NF-κB regulates the expression of stem cell markers such as *Lhx2* and *Sox9* (Tomann et al., 2016) and that NF-κB appears to be indispensable for stem cell activation, maintenance and/or growth in guard HF, it will be highly interesting to explore a potential role for NF-κB in stem cell biology of other epithelial appendages and tissues, as well as in cancer.

MATERIALS AND METHODS

Mice

Animal care and experimental protocols were approved by the Berlin Animal Review Board (Reg. G 0077/08, G 0082/13, G 0358/13 and X 9013/11). Mice were genotyped by genomic DNA PCR. See Supplementary Material for further detailed information.

Hair cycle analysis

Sagittal sections of mid-dorsal skin samples taken at indicated time points after depilation were analyzed according to (Muller-Rover et al., 2001). For quantification of hair types and calculation of hair cycle score (HCS), hair fiber and HF length see Supplementary Material. Statistical analysis was performed using unpaired Student's t-test.

Histology, X-Gal staining, immunofluorescence and *in situ* hybridization

Depilated back skin samples were fixed in 4% paraformaldehyde/MEM (immunofluorescence) or in Bouin's fixative (*in situ* hybridization) overnight at 4°C, dehydrated and paraffin-embedded. Routine H&E staining was done for morphological evaluation. Immunofluorescence and *in situ* hybridization on paraffin sections were performed as described (Zhang et al., 2009). For antibodies and *in situ* hybridization probes see Supplementary Material. DAPI was used for nuclear counterstain. For X-Gal staining, fresh tissue was embedded in TissueTek, and 5 – 10μm cryosections were treated as described (Zhang et al., 2009). Images were obtained using conventional or confocal Zeiss microscopes.

CONFLICT OF INTEREST

The authors state no financial or non-financial conflict of interest.

ACKNOWLEDGEMENTS

We thank Sandra Herms, Doris Lange, Alexandra Schulze, Lisa Spatt and Sarah Ugowski for excellent technical help and animal welfare and breeding, Michael Willenbrock for confocal microscopy and Ronald Naumann for transgenic mouse production. Furthermore, we thank Walter Birchmeier for providing *cond-lacZ* (*B6-Axin2*^{tm1Mdcb}) mice.

SUPPLEMENTARY MATERIAL

See online.

REFERENCES

Barker N, van Es JH, Kuipers J, Kujala P, van den Born M, Cozijnsen M, et al. Identification of stem cells in small intestine and colon by marker gene Lgr5. Nature 2007;449(7165):1003-7.

Bazzi H, Fantauzzo KA, Richardson GD, Jahoda CA, Christiano AM. The Wnt inhibitor, Dickkopf 4, is induced by canonical Wnt signaling during ectodermal appendage morphogenesis. Dev Biol 2007;305(2):498 - 507.

Chen CC, Wang L, Plikus MV, Jiang TX, Murray PJ, Ramos R, et al. Organ-level quorum sensing directs regeneration in hair stem cell populations. Cell 2015;161(2):277-90.

Chi W, Wu E, Morgan BA. Dermal papilla cell number specifies hair size, shape and cycling and its reduction causes follicular decline. Development 2013;140(8):1676-83.

Choi YS, Zhang Y, Xu M, Yang Y, Ito M, Peng T, et al. Distinct functions for Wnt/beta-catenin in hair follicle stem cell proliferation and survival and interfollicular epidermal homeostasis. Cell Stem Cell 2013;13(6):720-33.

Cui CY, Hashimoto T, Grivennikov SI, Piao Y, Nedospasov SA, Schlessinger D. Ectodysplasin regulates the lymphotoxin-beta pathway for hair differentiation. Proc Natl Acad Sci U S A 2006;103(24):9142-7.

Doffinger R, Smahi A, Bessia C, Geissmann F, Feinberg J, Durandy A, et al. X-linked anhidrotic ectodermal dysplasia with immunodeficiency is caused by impaired NF-kappaB signaling. Nat Genet 2001;27(3):277-85.

Elomaa O, Pulkkinen K, Hannelius U, Mikkola M, Saarialho-Kere U, Kere J. Ectodysplasin is released by proteolytic shedding and binds to the EDAR protein. Hum Mol Genet 2001;10(9):953-62.

Fantauzzo KA, Bazzi H, Jahoda CA, Christiano AM. Dynamic expression of the zinc-finger transcription factor Trps1 during hair follicle morphogenesis and cycling. Gene Expr Patterns 2008;8(2):51-7.

Fessing MY, Sharova TY, Sharov AA, Atoyan R, Botchkarev VA. Involvement of the Edar signaling in the control of hair follicle involution (catagen). Am J Pathol 2006;169(6):2075-84.

Fliniaux I, Mikkola ML, Lefebvre S, Thesleff I. Identification of dkk4 as a target of Eda-A1/Edar pathway reveals an unexpected role of ectodysplasin as inhibitor of Wnt signalling in ectodermal placodes. Dev Biol 2008;320(1):60-71.

Folgueras AR, Guo X, Pasolli HA, Stokes N, Polak L, Zheng D, et al. Architectural niche organization by LHX2 is linked to hair follicle stem cell function. Cell Stem Cell 2013;13(3):314-27.

Hammerschmidt B, Schlake T. Localization of Shh expression by Wnt and Eda affects axial polarity and shape of hairs. Developmental Biology 2007;305(1):246 - 61.

Hsu YC, Li L, Fuchs E. Transit-amplifying cells orchestrate stem cell activity and tissue regeneration. Cell 2014;157(4):935-49.

Ito M, Kizawa K, Toyoda M, Morohashi M. Label-retaining cells in the bulge region are directed to cell death after plucking, followed by healing from the surviving hair germ. J Invest Dermatol 2002;119(6):1310-6.

Jaks V, Barker N, Kasper M, van Es JH, Snippert HJ, Clevers H, et al. Lgr5 marks cycling, yet long-lived, hair follicle stem cells. Nat Genet 2008;40(11):1291-9.

Kadaja M, Keyes BE, Lin M, Pasolli HA, Genander M, Polak L, et al. SOX9: a stem cell transcriptional regulator of secreted niche signaling factors. Genes Dev 2014;28(4):328-41.

Kloepper JE, Ernst N, Krieger K, Bodo E, Biro T, Haslam IS, et al. NF-kappaB Activity Is Required for Anagen Maintenance in Human Hair Follicles In Vitro. J Invest Dermatol 2014;134(7):2036-8.

Monreal AW, Ferguson BM, Headon DJ, Street SL, Overbeek PA, Zonana J. Mutations in the human homologue of mouse dl cause autosomal recessive and dominant hypohidrotic ectodermal dysplasia [see comments]. Nat Genet 1999;22(4):366-9.

Mordmuller B, Krappmann D, Esen M, Wegener E, Scheidereit C. Lymphotoxin and lipopolysaccharide induce NF-kappaB-p52 generation by a co-translational mechanism. EMBO Rep 2003;4(1):82-7.

Mou C, Jackson B, Schneider P, Overbeek PA, Headon DJ. Generation of the primary hair follicle pattern. Proc Natl Acad Sci U S A 2006;103(24):9075-80. Epub 2006 Jun 12.

Muller-Rover S, Handjiski B, van der Veen C, Eichmuller S, Foitzik K, McKay IA, et al. A comprehensive guide for the accurate classification of murine hair follicles in distinct hair cycle stages. J Invest Dermatol 2001;117(1):3-15.

Myung PS, Takeo M, Ito M, Atit RP. Epithelial Wnt ligand secretion is required for adult hair follicle growth and regeneration. J Invest Dermatol 2013;133(1):31-41.

Nowak JA, Polak L, Pasolli HA, Fuchs E. Hair follicle stem cells are specified and function in early skin morphogenesis. Cell Stem Cell 2008;3(1):33-43.

Oshimori N, Fuchs E. Paracrine TGF-beta signaling counterbalances BMP-mediated repression in hair follicle stem cell activation. Cell Stem Cell 2012;10(1):63-75.

Plikus MV, Chuong CM. Macroenvironmental regulation of hair cycling and collective regenerative behavior. Cold Spring Harb Perspect Med 2014;4(1):a015198.

Plikus MV, Mayer JA, de la Cruz D, Baker RE, Maini PK, Maxson R, et al. Cyclic dermal BMP signalling regulates stem cell activation during hair regeneration. Nature 2008;451(7176):340-4.

Pummila M, Fliniaux I, Jaatinen R, James MJ, Laurikkala J, Schneider P, et al. Ectodysplasin has a dual role in ectodermal organogenesis: inhibition of Bmp activity and induction of Shh expression. Development 2007;134(1):117-25.

Reddy S, Andl T, Bagasra A, Lu MM, Epstein DJ, Morrisey EE, et al. Characterization of Wnt gene expression in developing and postnatal hair follicles and identification of Wnt5a as a target of Sonic hedgehog in hair follicle morphogenesis. Mech Dev 2001;107(1-2):69-82.

Rhee H, Polak L, Fuchs E. Lhx2 maintains stem cell character in hair follicles. Science 2006;312(5782):1946-9.

Schlake T. Segmental Igfbp5 expression is specifically associated with the bent structure of zigzag hairs. Mech Dev 2005;122(9):988-97.

Schlake T. Krox20, a novel candidate for the regulatory hierarchy that controls hair shaft bending. Mech Dev 2006;123(8):641-8. Epub 2006 Jun 6.

Schlake T. Determination of hair structure and shape. Semin Cell Dev Biol 2007;18(2):267-73.

Schmidt-Ullrich R, Aebischer T, Hulsken J, Birchmeier W, Klemm U, Scheidereit C. Requirement of NF-kappaB/Rel for the development of hair follicles and other epidermal appendices. Development 2001;128(19):3843-53.

Schmidt-Ullrich R, Memet S, Lilienbaum A, Feuillard J, Raphael M, Israel A. NF-kappaB activity in transgenic mice: developmental regulation and tissue specificity. Development 1996;122(7):2117-28.

Schmidt-Ullrich R, Tobin DJ, Lenhard D, Schneider P, Paus R, Scheidereit C. NF-kappaB transmits Eda A1/EdaR signalling to activate Shh and cyclin D1 expression, and controls post-initiation hair placode down growth. Development 2006;133(6):1045-57.

Schneider MR, Schmidt-Ullrich R, Paus R. The hair follicle as a dynamic miniorgan. Curr Biol 2009;19(3):R132-42.

Sharov AA, Sharova TY, Mardaryev AN, di Vignano AT, Atoyan R, Weiner L, et al. Bone morphogenetic protein signaling regulates the size of hair follicles and modulates the expression of cell cycle-associated genes. Proc Natl Acad Sci U S A 2006;103(48):18166-71. Epub 2006 Nov 17.

Smahi A, Courtois G, Rabia SH, Doffinger R, Bodemer C, Munnich A, et al. The NF-kappaB signalling pathway in human diseases: from incontinentia pigmenti to ectodermal dysplasias and immune-deficiency syndromes. Hum Mol Genet 2002;11(20):2371-5.

Sun SC. The noncanonical NF-kappaB pathway. Immunol Rev 2012;246(1):125-40.

Sundberg JP, Peters EM, Paus R. Analysis of hair follicles in mutant laboratory mice. J Investig Dermatol Symp Proc 2005;10(3):264-70.

Thibaut S, Gaillard O, Bouhanna P, Cannell DW, Bernard BA. Human hair shape is programmed from the bulb. Br J Dermatol 2005;152(4):632-8.

Tomann P, Paus R, Millar SE, Scheidereit C, Schmidt-Ullrich R. Lhx2 is a direct NF-kappaB target gene that promotes primary hair follicle placode down-growth. Development 2016;143(9):1512-22.

Tornqvist G, Sandberg A, Hagglund AC, Carlsson L. Cyclic expression of lhx2 regulates hair formation. PLoS Genet 2010;6(4):e1000904.

Vidal VP, Chaboissier MC, Lutzkendorf S, Cotsarelis G, Mill P, Hui CC, et al. Sox9 is essential for outer root sheath differentiation and the formation of the hair stem cell compartment. Curr Biol 2005;15(15):1340-51.

Yilmaz ZB, Kofahl B, Beaudette P, Baum K, Ipenberg I, Weih F, et al. Quantitative dissection and modeling of the NF-kappaB p100-p105 module reveals interdependent precursor proteolysis. Cell Rep 2014;9(5):1756-69.

Zhang Y, Tomann P, Andl T, Gallant NM, Huelsken J, Jerchow B, et al. Reciprocal requirements for EDA/EDAR/NF-kappaB and Wnt/beta-catenin signaling pathways in hair follicle induction. Dev Cell 2009;17(1):49-61.

FIGURE LEGENDS

Figure 1. NF-κB is active in all hair cycle phases. (**a)** Telogen HFs in *κ-Gal* (left panel) and *κ-EGFP* (right panel) mice before depilation (P53). (**b**) – (**d**) Sagittal sections of *κ-EGFP* reporter mice showing EGFP (**b**, **c**, **d**) and p65 (**d**) expression in anagen (**b**, **d**), catagen and telogen (**c**) HFs at indicated time points after depilation (d1, 3, 5, 16 and 21). Model below (**a**) and (**b**) summarizes NF-κB activity (red) during the hair cycle. Red arrows/arrowheads indicate NF-κB activity, green arrowhead (**d**) nuclear p65 expression, yellow arrowheads (**d**) co-localization of EGFP and nuclear p65 expression. APM, arrector pili muscle; B, bulge; DP, dermal papilla; HF KC, HF keratinocytes; IRS, inner root sheath; SG, sebaceous gland; SHG, secondary hair germ. Scale bars = 50μm (**a** – **c**), 100μM (**d**).

Figure 2. NF-κB activity co-localizes with known HF markers. (**a**) Sagittal sections of *κ-EGFP* reporter mice at d3 showing anagen I and II HFs stained with antibodies as indicated in each panel. (**b**) Sagittal section of *κ-EGFP* reporter mice at P53 (telogen) using antibodies against EGFP and LGR5. (**c**) Sagittal sections of *κ-EGFP* reporter mice at d5 stained with antibodies as indicated in each panel. Blue and green arrows/arrowheads indicate expression sites of the corresponding HF marker, red arrows/arrowheads mark NF-κB activity, and yellow arrows/arrowheads indicate co-localization of NF-κB activity with HF marker. B, bulge; DP, dermal papilla; SG, sebaceous gland; SHG, secondary hair germ; TACs, transit-amplifying cells. 400x magnification.

Figure 3. Delay in anagen development and hair cycle progression in *K5-ΔN* mice. (**a**) Hematoxylin-stained sagittal sections compare HFs at different stages of the hair cycle in *K5-ΔN* and control mice: d1 – d3, early anagen; d5, mid-anagen; d10, late anagen; d16, early

catagen; d18, mid-catagen; d25, telogen. (**b**) Quantification of HFs in distinct hair cycle phases and HCS analysis in *K5-ΔN* and control mice (see Supplementary Material for further information). (**c**) Schematic illustration shows delayed HF cycle progression in *K5-ΔN* mice when compared with controls. Scale bars = 50 μm. *; $p<0.05$, **; $p<0.01$, error bars = SEM. DP, dermal papilla; HS, hair shaft; IRS, inner root sheath.

Figure 4. *K5-ΔN* mice reveal shorter HFs and fibers. (**a**) Left panels: Ki67 staining on sagittal sections of *K5-ΔN* (n=2) and control mice (n=2) at d1. Scale bars = 50μm. Right panel: Quantification of Ki67+ cells/HF. *: $p<0.05$, error bars = SEM. **(b**) Ki67 staining on sagittal sections of *K5-ΔN* (n=2) and control mice (n=2) at d10. Scale bars = 50μm**.** (**c**) Hematoxylin-stained HFs (200x magnification) and HF length measurements of *K5-ΔN* (n=3) and control mice (n=3) at d5. *: $p<0.05$, error bars = SEM. (**d**) Plucked hairs (left panels) and measurements of hair fiber length (right panel) of *K5-ΔN* (n=2) and control mice (n=2) at d18. *: $p<0.05$, error bars = SEM. Scale bars = 0.5mm.

Figure 5. Non-canonical NF-κB signalling is required for hair shaft bending. (**a**) Plucked hairs at d18. (**b**) Awl/intermediate and zigzag hair quantification in *K5-ΔN* and control mice at d18, d21 and d25. *: $p<0.05$; ***: $p\leq0.001$; error bars = SEM. (**c**) In situ hybridization (ISH) using *Eda-A1*, *Nfkbia* (IκBα), *Shh*, *Wnt10b*, *Dkk4* and *Igfbp5* riboprobes on sagittal sections of *K5-ΔN* and control mice at d10. (**d**) Upper panels: RELB protein expression in anagen HFs of *K5-ΔN* and control mice. Lower panels: ISH with *RelB* riboprobe. (**e**) Overview of pelage hairs of untreated (control) and dox-treated *K5-RelB*$^{flox/flox}$ mice (*K5-RelB*$^{-/-}$) at d18. Black arrows indicate mRNA/protein expression. au = auchene, aw = awl, g = guard, z = zigzag, i = intermediate awl. Scale bars = 50μm. (**a**) and (**e**), 64x magnification.

Figure 6. *K5-ΔN* mice have decreased numbers of guard HFs. (**a**) Quantification of plucked hairs of *K5-ΔN* (n=7) and control mice (n=6) 18, 21 and 25 days after depilation. (**b**) Long-term dox treatment (6-7 months) without depilation of *K5-ΔN* (n=6) and untreated control mice (n=4) resulted in significantly reduced numbers of guard and zigzag hairs. (**c**) Images (left panels) and quantification (right panels) of guard HFs on Hematoxylin-stained sagittal sections of *K5-ΔN* (n=3) and control mice (n=3) at d5. 100x magnification. 40 sections/untreated or dox-treated *K5-ΔN* mouse were analyzed. Guard HFs were identified by shape and size. Note a significant reduction of guard HFs in *K5-ΔN* (30.6% ± 18.1%) vs. control mice (92.7% ± 8.0%). *: $p \leq 0.05$, **: $p \leq 0.005$, ***: $p \leq 0.0005$. Error bars = SEM.

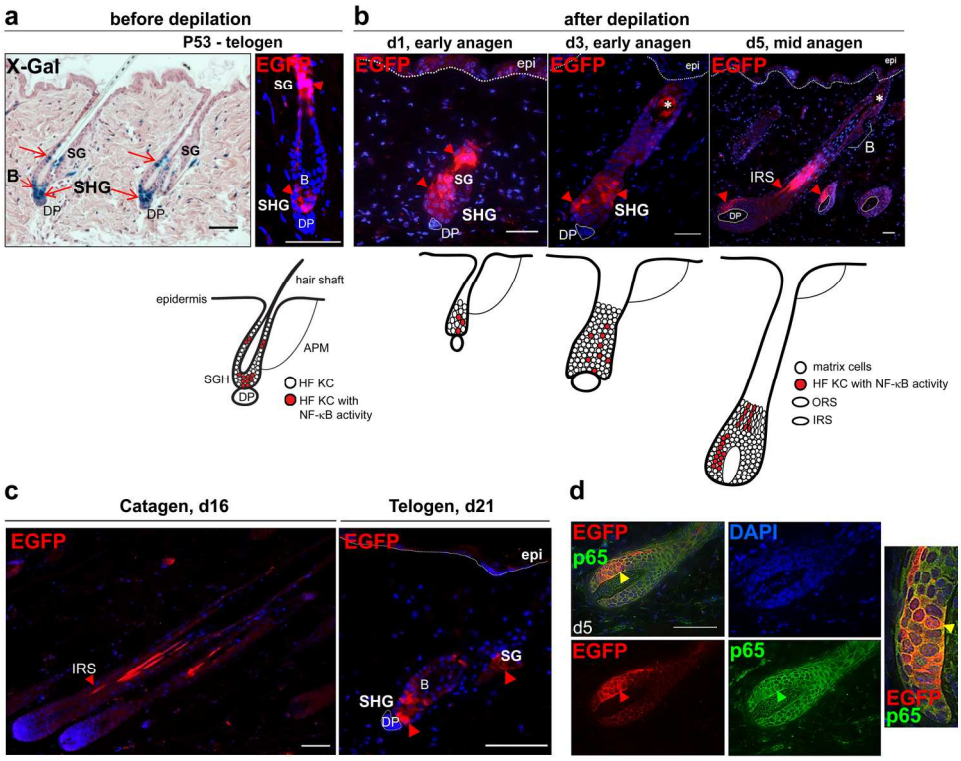

JID-2016-1017 Figure 1

186x144mm (300 x 300 DPI)

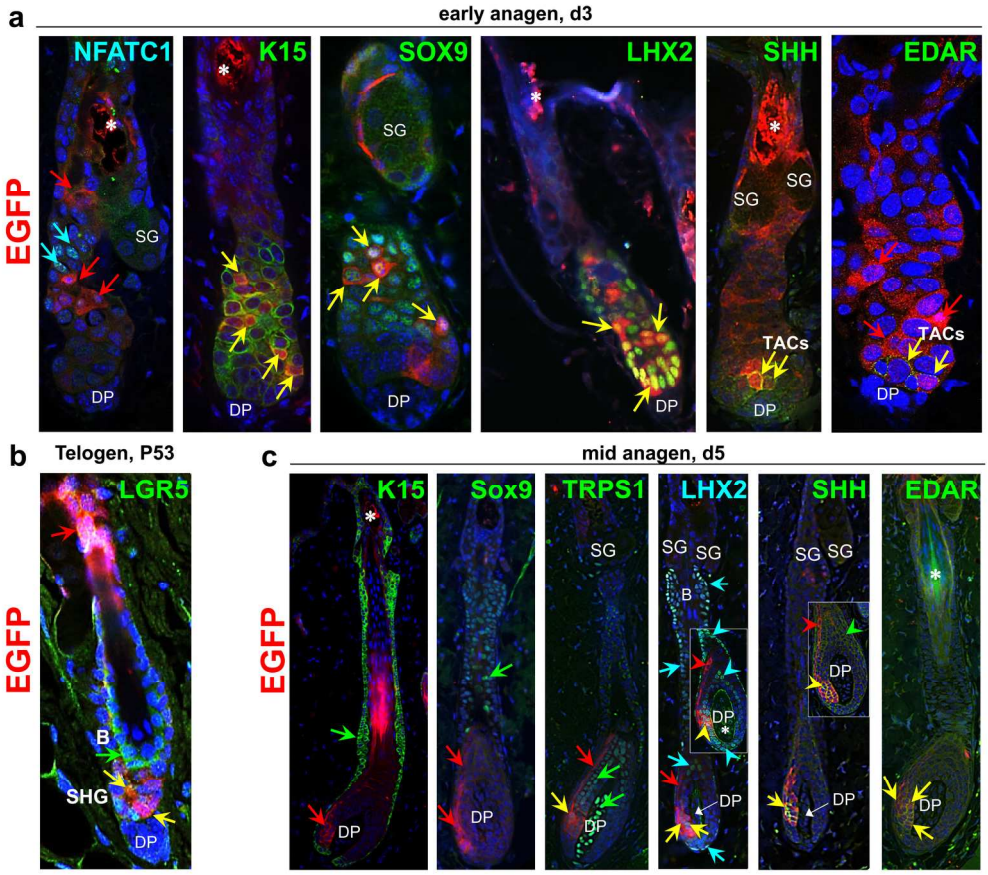

JID-2016-1017 Figure 2

190x167mm (300 x 300 DPI)

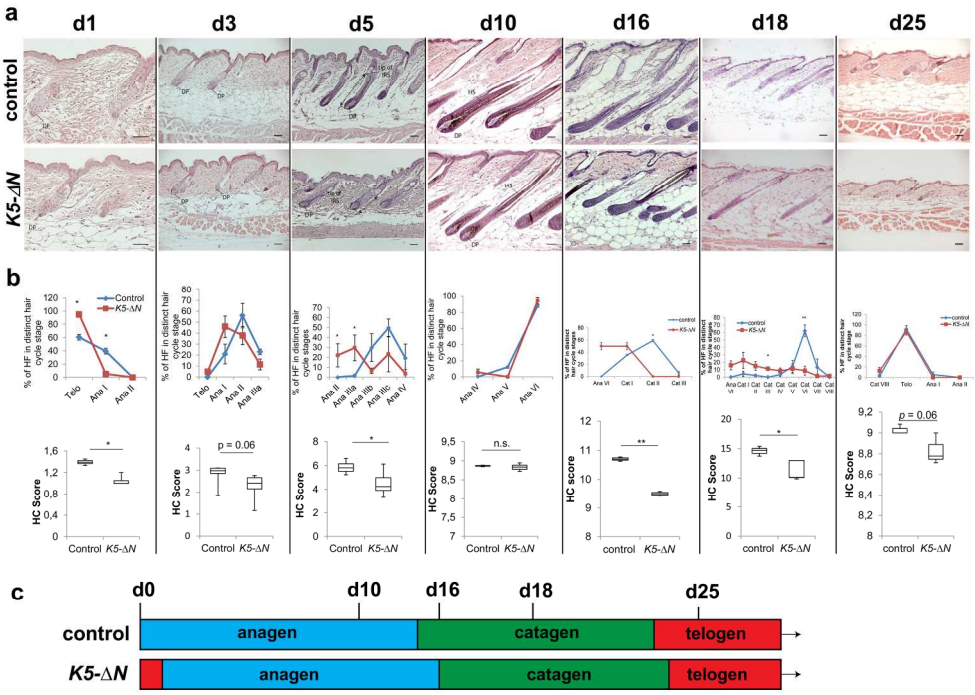

JID-2016-1017 Figure 3

205x148mm (300 x 300 DPI)

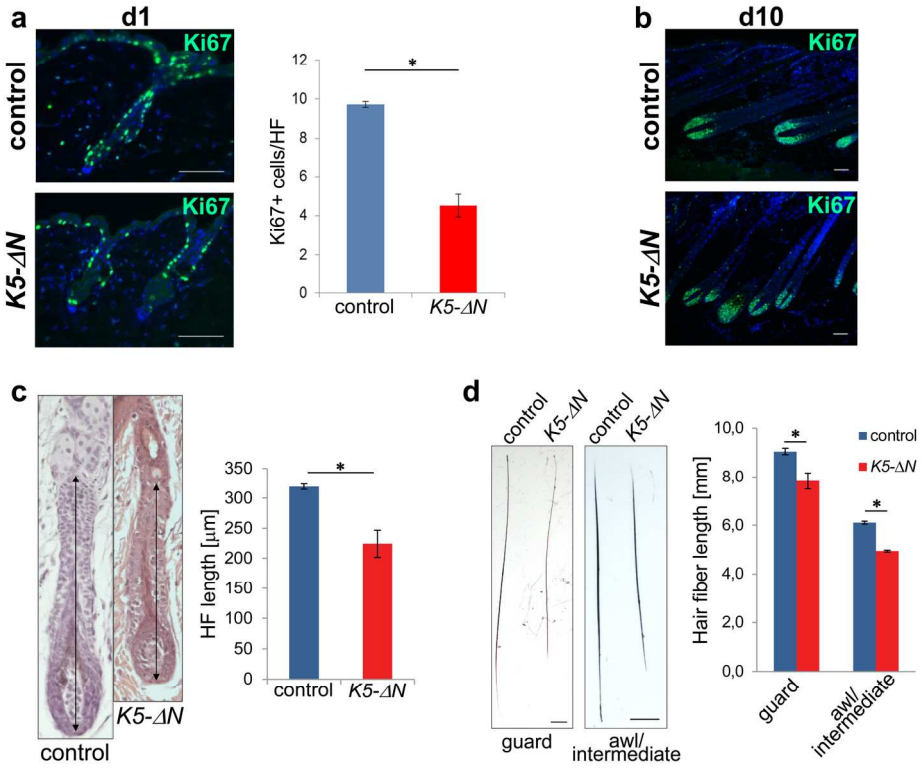

JID-2016-1017 Figure 4

177x146mm (300 x 300 DPI)

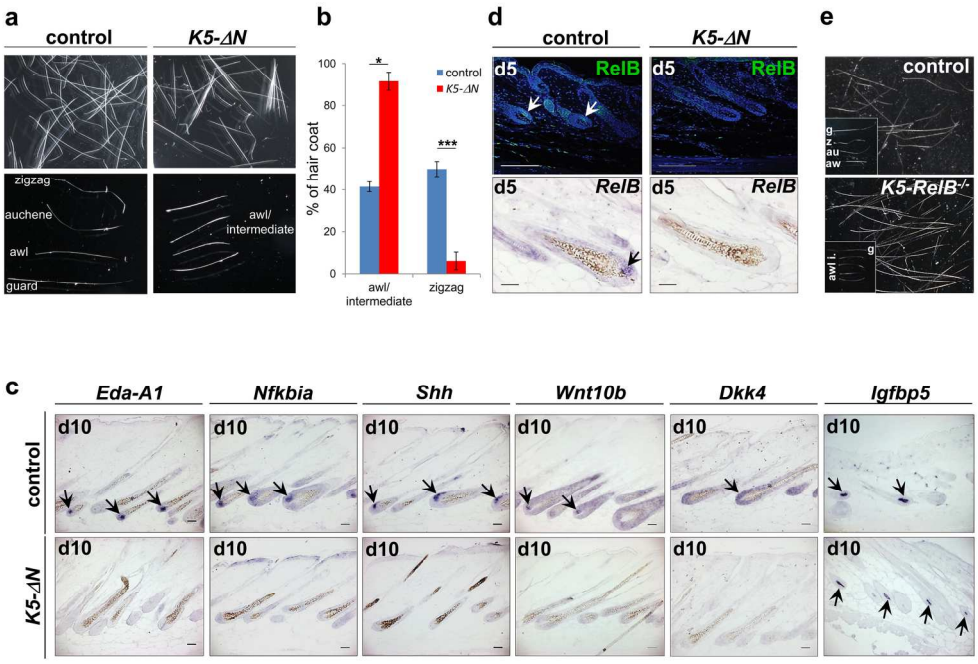

JID-2016-1017 Figure 5

181x131mm (300 x 300 DPI)

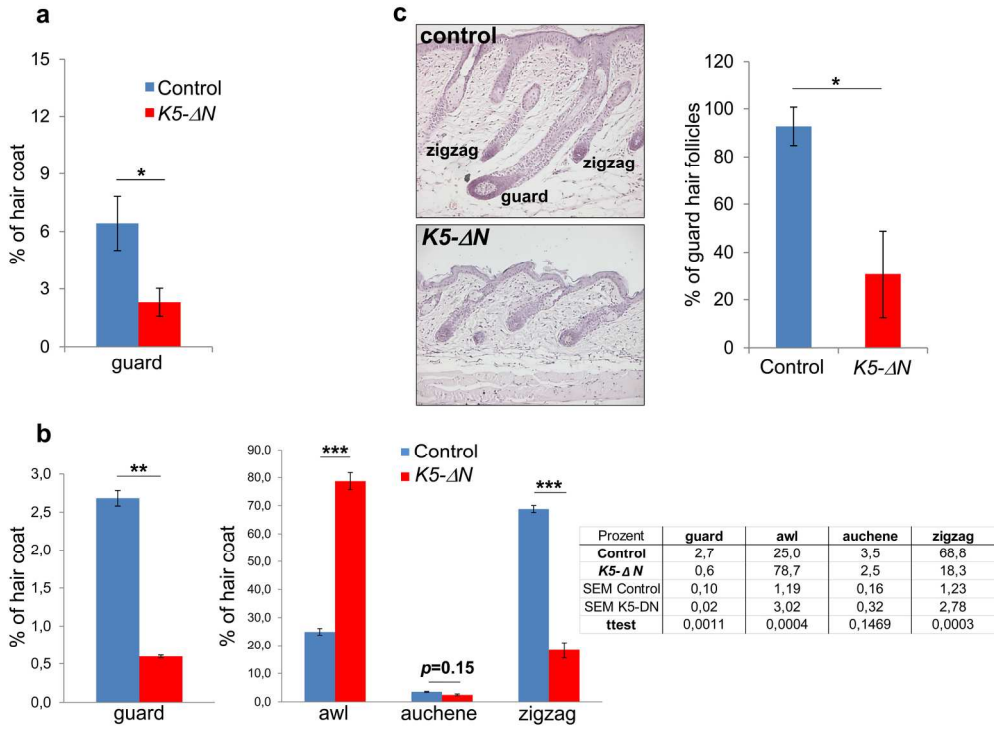

Prozent	guard	awl	auchene	zigzag
Control	2,7	25,0	3,5	68,8
K5-Δ N	0,6	78,7	2,5	18,3
SEM Control	0,10	1,19	0,16	1,23
SEM K5-DN	0,02	3,02	0,32	2,78
ttest	0,0011	0,0004	0,1469	0,0003

JID-2016-1017 Figure 6

190x146mm (300 x 300 DPI)

Supplementary Material

Supplementary Figures and Tables

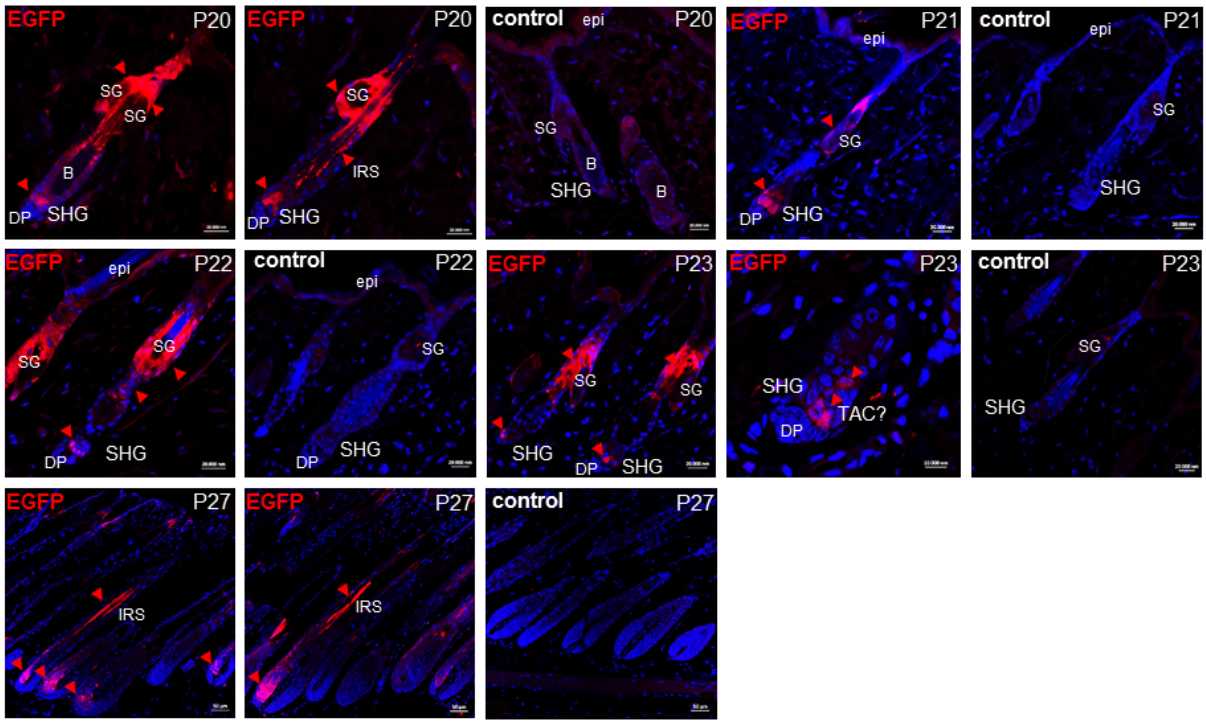

Supplementary Figure S1.

In the absence of depilation (natural hair cycle) NF-κB activity is also observed in the SHG, IRS and around the sebaceous gland. Represenative immunofluorescence images of sagittal sections of *κ-EGFP* reporter and control littermates (n=2/day/genotype) showing EGFP expression in late telogen (at P20), early anagen (at P21, 22 and 23) and mid-anagen (at P27) HFs. Scale bars for P20-P23 = 20μm; scale bar of middle panel of P23: 10μm; scale bars for P27 = 50μm. DP, dermal papilla; epi, epidermis; IRS, inner root sheath; SG, sebaceous gland; SHG, secondary hair germ; TAC, transit-amplifying cell. Note that NF-κB activity in the sebaceous gland area strongly diminished at mid-anagen.

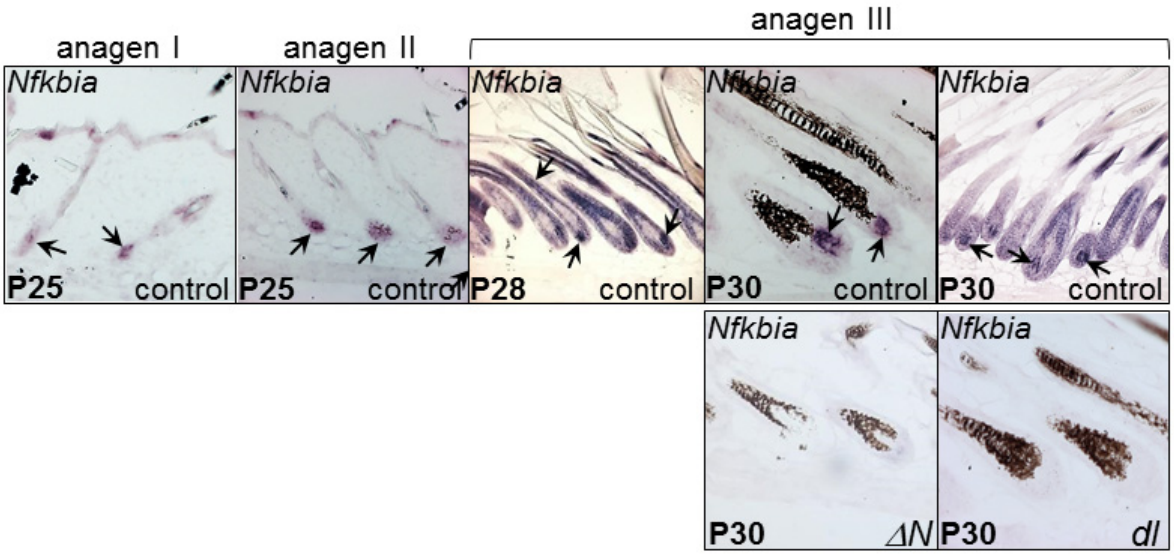

Supplementary Figure S2.

Further evidence for NF-κB activity in the murine hair follicle (HF). In situ hybridization on sagittal sections of *ΔN* (ubiquitously suppressed NF-κB activity; (Schmidt-Ullrich et al., 2001)), *Edar*-mutant (*dl*, *downless; B6C3Fe-a/a-Edar*$^{dl\text{-}j}$*/J*, obtained from Jackson Laboratories; see below in Supplementary Information, Material and Methods) and the corresponding littermate control mice (n=3 of each genotype and corresponding control) using an antisense riboprobe for the NF-κB target gene *Nfkbia* (IκBα) at indicated postnatal days (P25, P28 and P30). Arrows point to *Nfkbia* mRNA expression in SHG, hair bulb and IRS of controls. As expected, *Nfkbia* mRNA expression was absent in *ΔN* mice. 200x magnification.

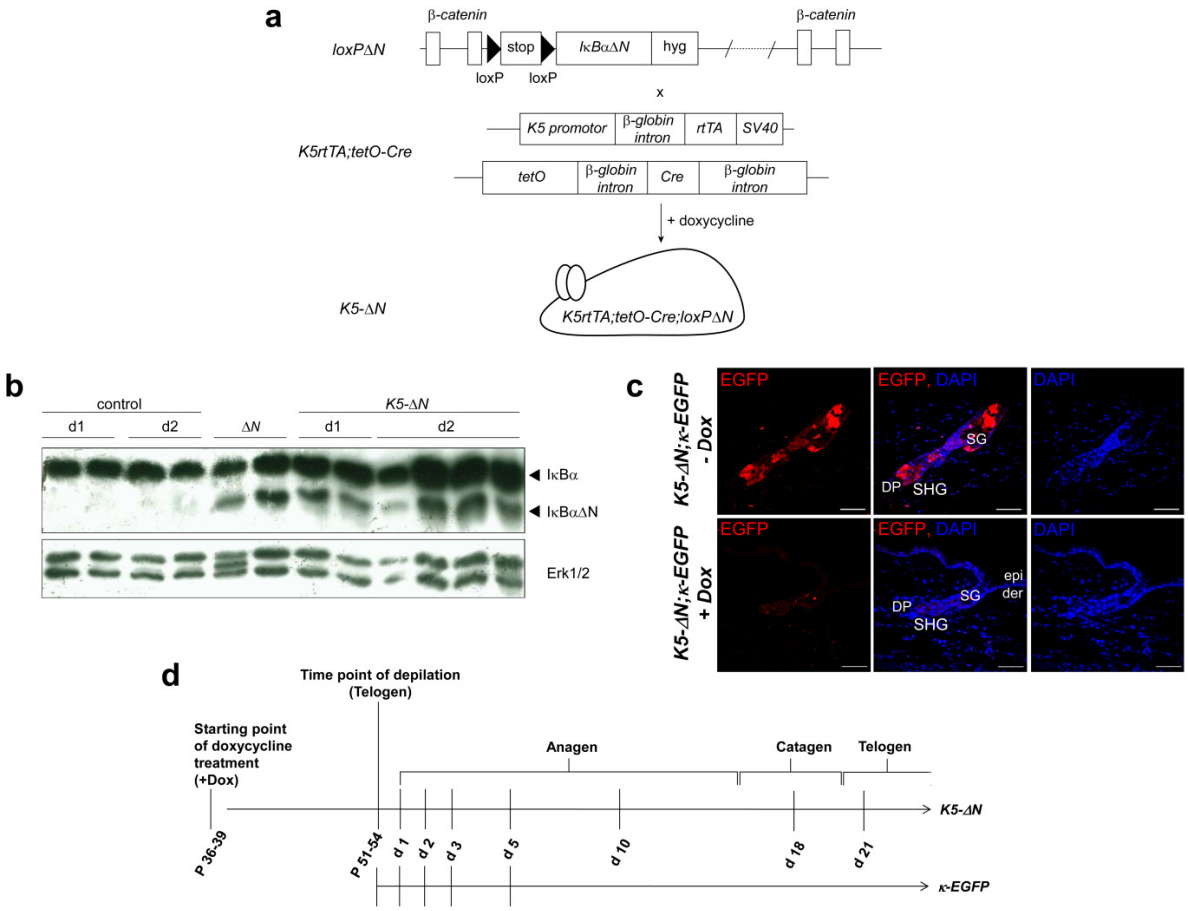

Supplementary Figure S3.

Inducible doxycycline (dox)-dependent NF-κB suppression in epithelial keratinocytes of adult mice. (**a**) Scheme for dox-inducible expression of super-repressor IκBαΔN. Double transgenic (*K5rtTA;tetO-Cre*) mice were mated with mice carrying a floxed *IκBαΔN* allele in the β-*catenin* locus (*ctnnb1*) (Schmidt-Ullrich et al., 2001). In triple transgenic offspring (*K5-ΔN*) Cre-mediated IκBαΔN expression is induced upon doxycycline (dox) treatment in epithelial keratinocytes. (**b**) Expression of IκBαΔN protein, which lacks 71 amino acids in the N-terminus (35kDa) was verified by Western blotting using whole skin extracts of dox-treated (referred to as ***K5-ΔN***) and untreated *K5-ΔN* mice (referred to as **control**) at different time points after

depilation (d1 and 2) and antibodies against C-term IκBα or ERK1/2 (control). Full length IκBα: 37kDa. n=2-4 *ΔN*, dox-treated and untreated *K5-ΔN* mice. (**c**) Representative immunofluorescence images of sagittal back skin sections of dox-treated and untreated (controls) *K5-ΔN;κ-EGFP* mice (n=3) 3 days after depilation using an anti-EGFP antibody (red) and nuclear DAPI staining. As expected, NF-κB activity was absent in HFs of dox-treated *K5-ΔN;κ-EGFP* mice when compared with untreated controls 3 days after depilation (early anagen). DP, dermal papilla; der, dermis; epi, epidermis; SG, sebaceous gland; SHG, secondary hair germ. (**d**) Outline of experimental design (see also main text and below).

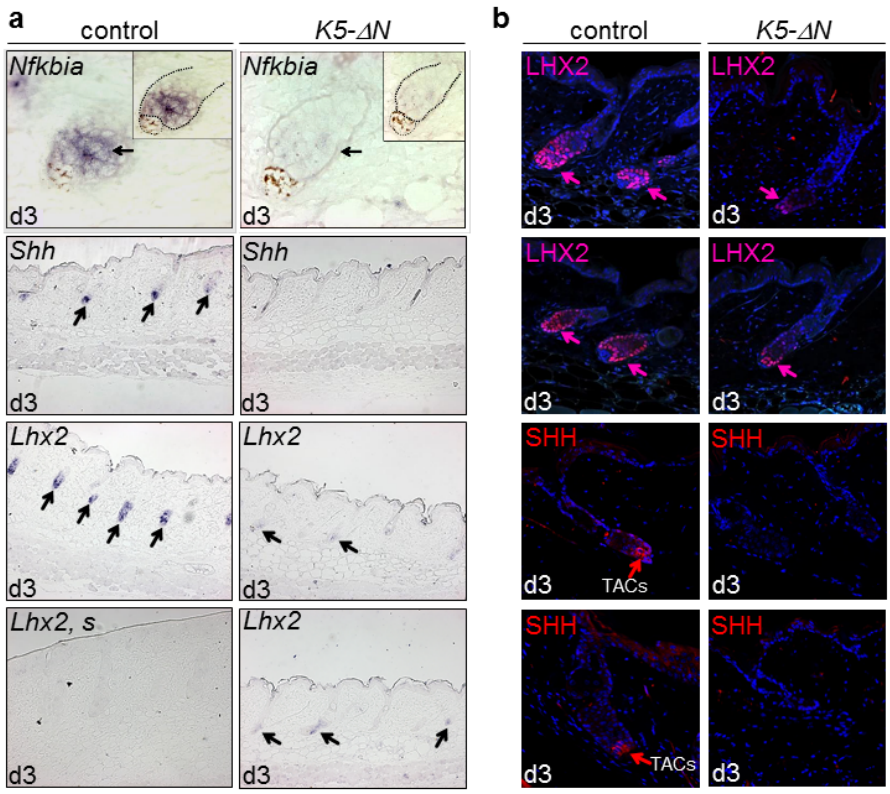

Supplementary Figure S4.

Further proof of suppressed NF-κB activity in epithelial keratinocytes of *K5-ΔN* mice: Strongly reduced or absent mRNA and protein expression of previously described NF-κB target genes *Nfkbia*, *Lhx2* and *Shh* (Schmidt-Ullrich et al., 2006, Tomann et al., 2016, Zhang et al., 2009)**.** (**a**) Representative images of in situ hybridization on sagittal back skin sections of dox-treated (*K5-ΔN*; n=3) and untreated (control; n=3) *K5-ΔN* mice 3 days after depilation (d3) using antisense riboprobes for *Nfkbia* (IκBα), *Shh* and *Lhx2*. As expected, the *Lhx2* sense riboprobe (*Lhx2*, s) did not hybridize. 100x, and 630x magnification (*Nfkbia*). Arrows point to *Nfkbia*, *Lhx2* and *Shh* mRNA expression in the SHG. Note that there still is very weak *Nfkbia* and some *Lhx2* mRNA expression in *K5-ΔN* mice (arrows). (**b**) Representative immunofluorescence images using an antibodies against LHX2 AND SHH on sagittal skin

sections of *K5-ΔN* (n=3) and control mice (n=3) 3 days after depilation (d3). 200x magnification. Arrows point to expression sites of LHX2 and SHH protein in the SHG. Reduced LHX2 or absent SHH protein expression in *K5-ΔN* mice corresponds to reduced *Lhx2* or strongly reduced *Shh* mRNA expression seen in (**a**).

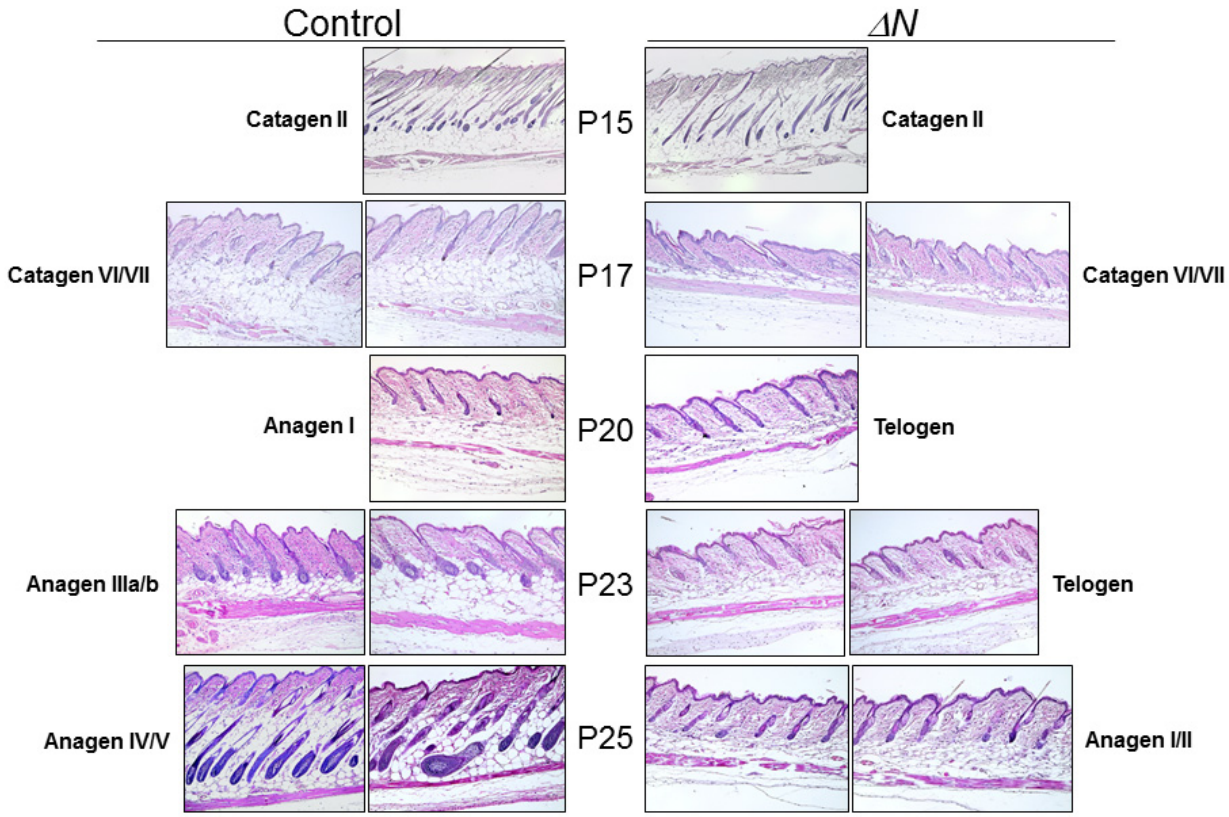

Supplementary Figure S5.

Natural anagen induction is also delayed in mice with ubiquitous suppression of NF-κB activity (*ΔN*) in the absence of depilation. Representative images of HE-stained back skin sections of *ΔN* mice (n=3) and control littermates (n=3) at indicated time points. P15: 50x magnification, P17 – P25: 100x magnification. Note that no differences were observed in catagen phase between *ΔN* mice and controls.

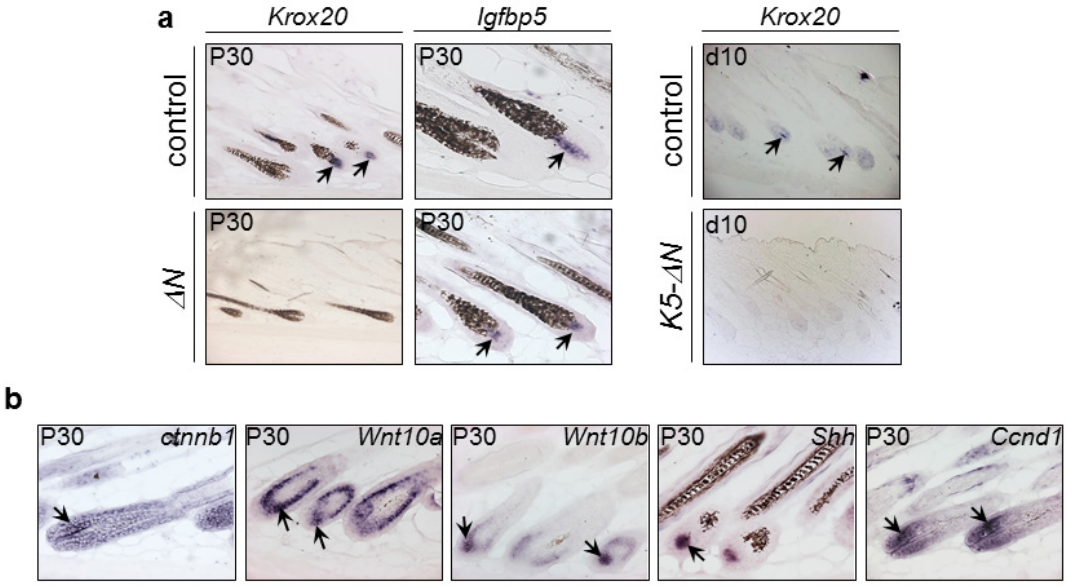

Supplementary Figure S6.

Expression analysis of HF bending markers. (**a**) In situ hybridization on sagittal back skin sections of *ΔN* and control littermates (n=3/3, control/*ΔN*) at postnatal day P30, and dox-treated (*K5-ΔN*) and untreated (control) *K5-ΔN* mice (n=3/3, control/*K5-ΔN*) 10 days after depilation (d10) using antisense riboprobes for *Krox20* and *Igfbp5*. 100x and 200x magnification. (**b**) mRNA expression of known direct (*Wnt10a*, *Wnt10b*, *Shh*) and indirect (*Ccnd1*) NF-κB target genes, as well as of β-catenin (*ctnnb1*) in full anagen follicles. In situ hybridization on sagittal back skin sections of wildtype mice (n=3) at P30 using antisense riboprobes as indicated. 200x magnification. Arrows point to *Krox20* and *Igfbp5* mRNA expression in the hair bulb.

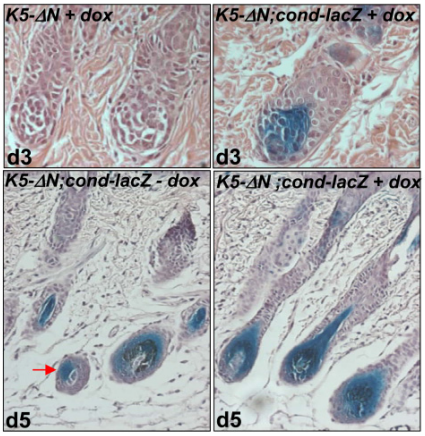

Supplementary Figure S7.

WNT signaling is still observed in *K5-ΔN* mice. Representative images of anagen follicles 3 (d3) and 5 (d5; mid-anagen) days after depilation. To detect WNT signaling, an X-Gal assay was performed on whole mount back skin samples from *K5-ΔN* (*K5-ΔN* + dox; negative control) as well as from offspring of matings between *K5-ΔN* and the WNT reporter line *cond-lacZ* (*K5-ΔN;cond-lacZ* + dox) mice and controls (*K5-ΔN;cond-lacZ* – dox). n=3 for each genotype. Following embedding in paraffin, sagittal sections were stained with Hematoxylin. Red arrow points to unilateral WNT activity in the hair bulb of untreated controls which is absent in dox-treated *K5-ΔN;cond-lacZ* mice. d3, 200x magnification; d5, 100x magnification

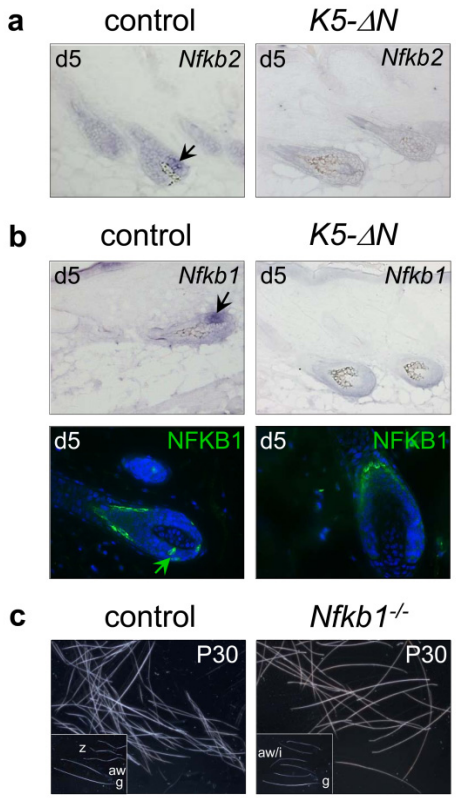

Supplementary Figure S8.

***K5-ΔN* and *Nfkb1-/-* mice lack zigzag hairs.** (**a**) In situ hybridization using an antisense riboprobe for *Nfkb2* (p100) on sagittal back skin sections of *K5-ΔN* and control mice 5 days after depilation (d5). 400x magnification. n=3/3 (control/*K5-ΔN*). (**b**) Upper panels, in situ hybridization with antisense riboprobe for *Nfkb1* (p105), and lower panels, representative immunofluorescence images with antibody against phospho-NFKB1 (p105) on sagittal back sections of *K5-ΔN* and control mice 5 days after depilation (d5). 400x magnification. n=3/3 (control/*K5-ΔN*). (**c**) Images of plucked hairs from *Nfkb1*$^{-/-}$ (p105 KO mice; see below) and control littermates. n=3 *Nfkb1*$^{-/-}$ and 3 controls. Similarly to *K5-RelB*$^{-/-}$ mice (see Figure 6e), *Nfkb1*$^{-/-}$ mice only revealed guard and awl-type hairs. Arrows point to *Nfkb1* and *Nfkb2* mRNA and NFKB1 protein expression in hair bulbs of controls.

Table S1. Hair cycle stages:

Days after depilation:	**d1** anagen I*	**d3** anagen II	**d5** anagen IIIa	**d10** late anagen	**d16** catagen I and II	**d18** mid-catagen, catagen VI	**d25** telogen
Untreated *K5-ΔN* (controls)	39% ± 4%	56% ± 11%	1% ± 1% in anagen IIIa. 99% HFs in anagen IV.	No difference.	100%, 60% in catagen II.	62% ± 8% in catagen VI	92% ± 7%
Dox-treated *K5-ΔN*	5% ± 4%	38% ± 8%	30% ± 13%	No difference	50% in anagen VI, and 50% in catagen I. 0% in catagen II.	20% in catagen I, 15% ± 5% in catagen II, 55-60% in catagen III – VI.	83% ± 6%
n (control/ *K5-ΔN*	2/4	3/3	4/6	2/2	2/2	3/4	3/3

*Hair cycle stage/s listed below days after depilation refer to the expected stage in control mice at the given time point.

Delayed anagen development and hair cycle progression in *K5-ΔN* mice. When compared with controls (untreated *K5-ΔN* mice), HFs in *K5-ΔN* (dox-treated *K5-ΔN*) mice showed a delay in anagen development and hair cycle progression after depilation, which was indicated by a peak shift in the percentage of HFs at a given hair cycle stage.

Table S2. Hair cycle score:

	d1, anagen I*	**d3**, anagen II	**d5**, anagen IIIa	**d10**, late anagen	**d16**, catagen I and II	**d18**, mid-catagen, catagen VI	**d25**, telogen
Untreated *K5-ΔN* (controls)	1.5 ± 0.03	3.0 ± 0.1	5.9 ± 0.1	8.88 ± 0.02	10.7 ± 0.05	14.6 ± 0.4	9.03 ± 0.04
Dox-treated *K5-ΔN*	1.08 ± 0.02	2.6 ± 0.2	4.6 ± 0.5	8.89 ± 0.08	9.5 ± 0.06	11.4 ± 0.7	8.83 ± 0.11
p-value	0.02	0.06	0.03	-	0.004	0.02	0.06

*Hair cycle stage/s listed below days after depilation refer to the expected stage in control mice at the given time point.

Reduced hair cycle score in *K5-ΔN* mice. The delay in anagen development and hair cycle progression in *K5-ΔN* mice after depilation was further endorsed by significantly reduced hair cycle scores (HCS) when compared to controls.

Supplementary Discussion and Observations

- Further remarks on the *K5-ΔN* mouse model (see also below: Material and Methods, Mouse lines): In our hands Cre deletion in the epidermis of *K5-ΔN* mice was >98% after 2 weeks feeding with doxycycline chow. This was tested by treating offspring of matings between *Tg(KRT5-rtTA-tetO-Cre)* and *B6;129S-Gtrosa26*^{tm1Sor} mice (obtained from Jackson Laboratories) with doxycycline at various lengths of time. A 15 day doxycycline treatment was required in order to express β-galactosidase in close to 100% epidermal and HF keratinocytes (K. K., data not shown).

However in all mouse models that harbor the NF-κB suppressor IκBαΔN (Krappmann et al., 1996), some residual NF-κB activity can still be detected. This is why constitutive and ubiquitous IκBαΔN expression (*ΔN* mice; see main text and Suppl. Material and Methods) is only embryonic lethal in about 25% of cases in contrast to complete NF-κB inhibition (Schmidt-Ullrich et al., 2001).

However, suppression by IκBαΔN appears to be sufficient in all cells/tissues that require NF-κB activity for development and maintenance. This is strongly supported by an identical phenotype of *ΔN* mice with mice lacking a functional TNF ligand EDA-A1 (*tabby*), or its receptor EDAR (*downless*), or EDARADD or Traf6 expression (Headon et al., 2001, Headon and Overbeek, 1999, Kere et al., 1996, Mikkola et al., 1999, Naito et al., 2002, Yan et al., 2002), or with mice lacking secondary lymph nodes and Peyer`s patches (*Aly/Aly* (*Nik* (NF-κB-inducing kinase) KO), *Ltβ* KO, *RelB* KO; (Alimzhanov et al., 1997, Fagarasan et al., 2000, Shinkura et al., 1999, Yilmaz et al., 2003, Yin et al., 2001)).

IκBαΔN has been knocked into the *β-catenin* (*Ctnnb1*) locus (Schmidt-Ullrich et al., 2001). Therefore the amount of IκBαΔN expression depends on the expression of *β-catenin* in a

particular tissue. In the epidermis and in HFs *β-catenin*, and thus IκBαΔN, are highly expressed (R. S.-U., unpublished data).

Nevertheless, it cannot be ruled out entirely that the HF phenotype observed in inducible *K5-ΔN* mice might have been more intensive in a setting of complete suppression of NF-κB activity. The hair cycle defect (delayed anagen entry) is more pronounced in *ΔN* mice when compared to dox-treated *K5-ΔN* mice (compare Figure 3 and Supplementary Figure S5).

- Further remarks on NF-κB activity in cycling HFs in connection with a possible function: NF-κB is not activated in quiescent HFSCs (no co-staining with NFATc1, see Figure 2a) and is thus not involved in HFSC maintenance. This suggests that lack of guard HF cycling/maintenance in dox-treated *K5-ΔN* mice is rather due to halted cell proliferation in the SHG, and/or premature maturation of SHG cells and/or lack of proper TAC functions (see below). Note that in early guard HF development NF-κB negatively regulates BMP signaling in order to prevent premature differentiation of placode keratinocytes (Mou et al., 2006) which may also apply to the SHG of guard HFs but needs further investigation.

The delayed anagen entry observed in awl/auchene and zigzag HF may be due to a retarded onset in SHG cell proliferation, which in *K5-ΔN* mice picks up at a later time point when compared to controls (see Figure 4). This may be a direct or indirect effect of suppressed NF-κB activity. We have previously shown that in early HF development, placode keratinocyte proliferation is dependent on, but not directly regulated by NF-κB (Schmidt-Ullrich et al., 2006, Tomann et al., 2016, Zhang et al., 2009). This may also be true for the SHG.

Note that NF-κB activity is not detected in all SHG germ cells. This is the reason why not all K15 or SOX9 expressing cells show simultaneous staining for EGFP. The reason for this remains unknown, but suggests specific functions for NF-κB in only a subset of the proliferating HFSC progeny in the SHG. However, for LHX2 and EGFP expression we saw a significant overlap (see Figure 2a; see also below).

- Further remarks on NF-κB target genes in mature HFs (Fig. 5, S3, S4): The expression of three previously identified NF-κB target genes in HF development, *Nfkbia* (Le Bail et al., 1993, Schmidt-Ullrichet al., 2006), *Shh* (Pummila et al., 2007, Schmidt-Ullrich et al., 2006, Tomann et al., 2016) and *Lhx2* (Tomann et al., 2016), was analyzed in early anagen HFs to further support efficient suppression of NF-κB activity in the epidermis of doxycycline-treated *K5-ΔN* mice (Supplementary Figure S4). The results suggest that NF-κB may also partially regulate *Shh* and *Lhx2* gene expression in mature cycling follicles (Supplementary Figure S4). However, although anagen induction is delayed in *K5-ΔN* mice, the HF cycle of awl and zigzag HFs proceeds normally once anagen is established. This indicates that the reduced levels of LHX2 expression are sufficient to allow normal hair cycle progression in *K5-ΔN* mice. Absent SHH expression in the HF bulb 3 days after depilation (d3; Supplementary Figure S4) appears to be overcome by other signals, at least in awl/auchene and zigzag follicles. However, lack of SHH expression in TACs may be detrimental for guard HFs (see below).

- EDA-A1/EDAR/NF-κB signaling in the hair cycle: EDA-A1/EDAR signaling directly controls canonical NF-κB activity during early primary guard hair follicle development (Schmidt-Ullrichet al., 2006). The role of EDA-A1/EDAR signaling in the adult hair cycle has not been

sufficiently analyzed to allow any clear-cut conclusions. However it has been shown that ligand and receptor are expressed in mature HFs (Elomaa et al., 2001, Fessing et al., 2006), which is confirmed in the present study. Furthermore, in *downless* mice (*Edar*-mutant mice) catagen entry appeared to be accelerated due to premature apoptosis in the outer rout sheath (ORS) (Fessing et al., 2006).

Here we show overlapping EDAR and EGFP expression only in the TAC area (see below) and unilaterally in the hair bulb at full anagen, concomitant with hair shaft bending markers (see main text). In contrast to Fessing et al. (Fessing et al., 2006), we did not observe any significant NF-κB activity at catagen. This may explain why we did not see accelerated catagen entry or increased apoptosis in mice with suppressed NF-κB activity. Catagen also appeared to proceed normally in *ΔN* mice (Supplementary Figure S5). Thus, it remains unknown how EDAR signaling regulates catagen entry.

Finally, we did not see any EDAR expression in the SHG at any time point. Hence, the signal that is responsible to regulate NF-κB activity in anagen development has also yet to be identified.

- Possible function for NF-κB in guard HF TACs? TACs are an intermediate phase between undifferentiated stem cells and differentiating cells. It was previously shown that HF TACs express SHH which is required for induction of quiescent stem cell proliferation (Hsu et al., 2014). In the absence of SHH activity in the epithelial part of the HF, the SHG and TAC population diminishes enormously and HF regeneration is blocked (Hsu et al., 2014). Our data suggests that EDA-A1/EDAR/NF-κB may regulate SHH expression in the TAC (see Figure 2 and S4). However, as discussed in the main text, this hypothetical function most likely would be limited to guard hair follicles which do no longer cycle in the absence of epidermal NF-κB

suppression. In the other HF types it must be overcome by other signals. These highly interesting findings need to be analyzed in more detailed in the future.

Our findings that suggest that EDA-A1/EDAR/NF-κB regulates SHH expression in TACs might also be interesting from another point of view: A recent publication showed that SHH signaling in TACs was responsible for dermal adipocyte production (dermal adipogenesis) (Zhang et al., 2016). During the hair cycle various changes in the surroundings of the cycling follicle take place, including expansion of adipose tissue during anagen phase. This appears to be controlled by SHH produced in TACs, as loss of *Shh* expression in TACs revealed loss of HF growth and concomitant dermal adipogenesis (Zhang et al., 2016). We have observed a reduction in adipose tissue in dox-treated *K5-ΔN* mice and particularly in adult *ΔN* mice (K. K. and R. S.-U., unpublished data). Thus, absent or strongly reduced SHH expression in HF TACs of *ΔN* and *K5-ΔN* mice may not only be responsible for reduced HF growth but also for reduced adipose tissue formation, which will be a further future project.

Supplementary Material and Methods

Mouse lines, generation of lines, doxycycline treatment, depilation

B6-Tg(κ-EGFP)3Pt/Rsu (*κ-EGFP*) and *B6-Tg(κ-Gal)3Rsu* (*κ-Gal*) NF-κB reporter lines, as well as mice with ubiquitously suppressed NF-κB activity *129;129P2-ctnnb1*$^{tm(NFKBIA\Delta N)1Rsu}$ (Δ*N*), *Nfkb1*$^{-/-}$ (*B6;129P2-Nfkb1*^{tm1Bal}*/J*, obtained from Jackson Laboratories), *B6C3Fe-a/a-Edar*$^{dl\text{-}j}$*/J* (*dl*, *downless*, obtained from Jackson Laboratories) and the WNT reporter line *cond-lacZ* (*B6-Axin2*^{tm1Mdcb}, kindly provided by Walter Birchmeier, MDC, Berlin, Germany) were described previously (Headon and Overbeek, 1999, Schmidt-Ullrich et al., 2001, Schmidt-Ullrich et al., 1996, Sha et al., 1995, Tomann et al., 2016, Yu et al., 2005). *K5-ΔN* mice were generated by mating *Tg(KRT5-rtTA-tetO-Cre)* ((Diamond et al., 2000, Mucenski et al., 2003); see also (Chu et al., 2004, Zhang et al., 2008)) with *129;129P2-ctnnb1*$^{tm(NFKBIA\Delta Nfl/fl)RSU}$ mice (*loxP*Δ*N*; (Henke et al., 2007, Marko et al., 2016, Schmidt-Ullrich et al., 2001)). *K5-RelB*$^{flox/flox}$ mice were produced by mating *Tg(KRT5-rtTA-tetO-Cre)* with *RelB*^{tm1Weih} (RelBflox) mice, a generous gift of Falk Weih, FLI for Age Research, Jena, Germany (Powolny-Budnicka et al., 2011).

For tetracycline-inducible NF-κB suppression or RelB deletion in epithelial keratinocytes, *K5-ΔN* or K5-RelB$^{flox/flox}$ mice were placed on doxycycline (dox) chow (6g/kg, Bio-Serv or Plexx B.V.) for 15 days starting at postnatal day 36 - 39 (P36 – 39; see Supplementary Figure 2d). Note that dox-treated *K5-RelB*$^{flox/flox}$ mice are designated as *K5-RelB*$^{-/-}$ mice throughout the text.

For long-term treatments with doxycycline chow, feeding was also started at P36 and was continued for 6-7 months without interruption before animals were analyzed for pelage hair composition. These mice were not depilated.

Depilation of back skin was performed around postnatal day P53 when hair follicles reside in telogen. Prior to depilation, mice were anesthetized with an air mixture containing 2% isoflurane

(Abbott). Back skin was depilated three times with cold wax stripes (Isana).

For every experiment/time point n = 2-7 mice of the corresponding genotype and their controls were used (for details see also Figure legends).

Western Blotting

Freshly isolated back skin was shock frozen in liquid nitrogen and was pulverized using a mortar. The pulverized skin was incubated in 300 µl lysis buffer (50mM Tris, 150mM NaCl, 1% NP-40, 1% Trition-X 100, 1µM MG-132) for 5 h on a rotating table. Sample was centrifuged for 20 min at 13.000 rpm. The supernatant was used for western blotting analysis. Antibodies used for Western blotting: IκBα, rabbit, Santa Cruz (sc-371) 1:1000; Erk1/2, rabbit, Cell Signaling (137F5) 1:1000.

Calculation of the hair cycle score (HCS)

To facilitate the correct assignment of all hair cycle stages (anagen I-VI, catagen I-VIII, telogen), the HCS was calculated for each HF in a histological section. To perform this analysis, every hair cycle stage is assigned a factor in ascending numerical order, e.g. 1 = telogen, 2 = anagen I, 3 = anagen III, 4 - 6 = anagen IIIa - c, 7 = anagen IV, 8 = anagen V, 9 = anagen VI, 10 = catagen I, 11 = catagen II, 12 = catagen III, 13 = catagen IV, 14 = catagen V, 15 = catagen VI, 16 = catagen VII, 17 = catagen VIII. The number of HFs in a particular hair cycle stage is multiplied by the corresponding factor. The result is divided by the total number of HFs counted (Muller-Rover et al., 2001). Additionally, the percentage of HFs in distinct hair cycle stages was calculated for dox-treated *K5-ΔN* mice and untreated controls. For every analyzed time point a minimum of three biological replicates were used for each group ($n \geq 3$).

Quantification of pelage hair types and calculation of hair fiber and HF length in control and *K5-ΔN* mice

For **Figure 5a and b, and 6a**: To quantify pelage hair types and calculate fiber length, pelage hairs were plucked from mid-dorsal skin of untreated (controls; total n=6) or dox-treated *K5-ΔN* (*K5-ΔN*; total n=7) mice 18 (n=2/2; controls/*K5-ΔN*), 21 (n=2/3) and 25 (n=2/2) days after depilation. To define the percentage of each hair type, a minimum of n = 100 randomly taken hair fibers were counted. The number of each hair type/total number of counted hairs was calculated. This led to the following numbers of zigzag and awl hairs: Zigzag hairs: 50.0% ± 3.6% (controls) vs. 6.2% ± 4.2% (*K5-ΔN*). Awl-type hairs: 41.5% ± 2.4% (controls) vs. 91.5% ± 4.3% (*K5-ΔN*).

For **Figure 6b**: After 6-7 months pelage hairs were plucked from mid-dorsal skin of untreated (controls; n=4) or dox-treated *K5-ΔN* (*K5-ΔN*; n=6) mice. To define the percentage of each hair type, n = 300 randomly taken hair fibers were counted. Calculations were performed as above.

For **Figure 6c**: Quantification of guard HFs on hematoxylin-stained sagittal back skin sections was preformed by counting n = 40 sections/per mouse/genotype. n =3 mice per genotype: 3 dox-treated *K5-ΔN* mice and 3 untreated controls. Guard HFs were identified by shape and size. All guard HFs identified in one section were counted.

N = 20 hair fibers/mouse were measured to calculate hair fiber length. Hairs in *K5-ΔN* mice were significantly shorter: 7.8 mm ± 0.3 mm vs. 9.1 mm ± 0.1 mm (controls) for guard hairs (p = 0.006), 4.9 mm ± 0.0 mm vs. 6.1 mm ± 0.1 mm (controls) for awl/intermediate hairs (p = 0.009).

To define the HF length, sagittal back skin sections of dox-treated *K5-ΔN* (n=3) and untreated control mice (n=3) 5 days after depilation were analyzed under the light microscope. To calculate the HF length, the distance between proximal HF bulb and the lower tip of the sebaceous gland

was measured (see Figure 4c). For each sample a number of n = 20 HF was measured. To measure the HF length, the ruler plugin software (Zeiss Axio Imager) was used. The mean values were calculated in Excel, and the unpaired Student's t-test was used to calculate the *p*-value. A significant *p*-value was set for $p \leq 0.05$. Follicles in *K5-ΔN* mice were significantly shorter: 224µm ± 23 µm vs. 319 µm ± 4 µm (controls), ($p = 0.04$).

Quantification of Ki67-positive cells in early anagen HFs

To quantify the number of Ki67-positive cells at d1 after depilation (see **Fig. 4a**), all Ki67-positive cells in the epithelial part of the HF between dermal papilla and sebaceous gland (= the cycling part) were counted in a total of 20 HFs/mouse. The average number of Ki67-positive cells/HF was then calculated. n=2 dox-treated *K5-ΔN* and n=2 untreated controls were used:

	Control	K5-DN
	9,95	3,7
	9,5	5,35
Mean	9,725	4,525
SD	0,225	0,825
n	2	2
(n)	1,41421356	1,41421356
SEM	0,15909903	0,58336309
ttest		0,04

In situ hybridization probes

In situ hybridization was carried out using the following mouse cDNA probe templates: *Eda-A1*, (Ectodysplasin-A1; nt 59 – 603; Y13438), *Shh* (nt 120 – 760; X76290) and *Ctnnb1* (β-catenin; nt 150 – 540; NM_007614), all kindly provided by Joerg Huelsken/W. Birchmeier, MDC, Berlin, Germany; *Nfkbia* (IκBα; nt 1 – 1091; U36277/NM010907); *Krox20* (zinc finger transcription factor, *Egr2*; nt 1 – 2742; BC009093); *Igfbp5* (insulin-like growth factor binding protein 5; nt 1 –

2192; BC057447); *Ccnd1* (cyclin D1; nt 931 – 2358; BC044841); *Lhx2* (nt 1 – 1891; BC055741); *Nfkb1* (p105; N-terminal 1.3 Kb, NM_008689); *Nfkb2* (p100; nt 274 – 1489; AF155373) and *Relb* (nt 1 – 2041; BC034523;), both kindly provided by F. Weih, FLI, Jena, Germany; *Dkk4* (Dickkopf 4; nt 77 – 837; NM_145592); *Wnt10a* (nt 1295 – 2487; U61969); *Wnt10b* (nt 735 – 2066; U61970).

Antibodies and dilutions used

The literature is referring to the identification and functions of the respective proteins in the murine hair cycle. A role for canonical NF-κB subunits p65 (RelA) and NFKB1 (p50) or for non-canonical RelB in hair cycling has not yet been identified.

- Digoxigenin-AP Fab fragments, sheep, Roche (11093274910) 1:1000,
- EDAR (Ectodysplasin receptor), goat, R&D Systems (AF745) 1:100, (Schmidt-Ullrich and Paus, 2005),
- EGFP, chicken, Abcam (ab13970) 1:400,
- Ki67, rabbit, Abcam (ab15580) 1:100,
- LGR5 (leucine-rich G protein–coupled receptor 5), rabbit, Novus Biologicals (NBP1-28904) 1:100, (Barker et al., 2007),
- LHX2 (LIM homeobox protein 2), goat, Santa Cruz (sc-19344) 1:100, (Folgueras et al., 2013, Rhee et al., 2006, Tornqvist et al., 2010),
- Keratin15 (K15), Abcam (ab52816) 1 :100, (Liu et al., 2003),
- NFATc1 (nuclear factor of T-cell C1), rabbit, Santa Cruz (sc-13033) 1:100, (Horsley et al., 2008),
- p65 (= RelA), rabbit, Santa Cruz (sc-372) 1:100,
- phospho-NFKB1 (= phospho-p105), rabbit, Cell Signaling (4806) 1:100,

- RelB, rabbit, Santa Cruz (sc-226, C-19) 1:100,
- SHH (sonic hedgehog), rabbit, Santa Cruz (sc-9024) 1:100, (Hsu et al., 2014, St-Jacques et al., 1998),
- SOX9 (SRY-box 9), rabbit, Santa Cruz (sc-20095) 1:100, (Nowak et al., 2008, Vidal et al., 2005),
- TRPS1 (trichorhinophalangeal syndrome 1), goat, Santa Cruz (sc-26974) 1:100, (Fantauzzo et al., 2008, Momeni et al., 2000).

Supplementary References

Alimzhanov MB, Kuprash DV, Kosco-Vilbois MH, Luz A, Turetskaya RL, Tarakhovsky A, et al. Abnormal development of secondary lymphoid tissues in lymphotoxin beta-deficient mice. Proc Natl Acad Sci U S A 1997;94(17):9302-7.

Barker N, van Es JH, Kuipers J, Kujala P, van den Born M, Cozijnsen M, et al. Identification of stem cells in small intestine and colon by marker gene Lgr5. Nature 2007;449(7165):1003-7.

Chu EY, Hens J, Andl T, Kairo A, Yamaguchi TP, Brisken C, et al. Canonical WNT signaling promotes mammary placode development and is essential for initiation of mammary gland morphogenesis. Development 2004;131(19):4819-29. Epub 2004 Sep 1.

Diamond I, Owolabi T, Marco M, Lam C, Glick A. Conditional gene expression in the epidermis of transgenic mice using the tetracycline-regulated transactivators tTA and rTA linked to the keratin 5 promoter. J Invest Dermatol 2000;115(5):788-94.

Elomaa O, Pulkkinen K, Hannelius U, Mikkola M, Saarialho-Kere U, Kere J. Ectodysplasin is released by proteolytic shedding and binds to the EDAR protein. Hum Mol Genet 2001;10(9):953-62.

Fagarasan S, Shinkura R, Kamata T, Nogaki F, Ikuta K, Tashiro K, et al. Alymphoplasia (aly)-type nuclear factor kappaB-inducing kinase (NIK) causes defects in secondary lymphoid tissue chemokine receptor signaling and homing of peritoneal cells to the gut-associated lymphatic tissue system. J Exp Med 2000;191(9):1477-86.

Fantauzzo KA, Bazzi H, Jahoda CA, Christiano AM. Dynamic expression of the zinc-finger transcription factor Trps1 during hair follicle morphogenesis and cycling. Gene Expr Patterns 2008;8(2):51-7.

Fessing MY, Sharova TY, Sharov AA, Atoyan R, Botchkarev VA. Involvement of the Edar signaling in the control of hair follicle involution (catagen). Am J Pathol 2006;169(6):2075-84.

Folgueras AR, Guo X, Pasolli HA, Stokes N, Polak L, Zheng D, et al. Architectural niche organization by LHX2 is linked to hair follicle stem cell function. Cell Stem Cell 2013;13(3):314-27.

Headon DJ, Emmal SA, Ferguson BM, Tucker AS, Justice MJ, Sharpe PT, et al. Gene defect in ectodermal dysplasia implicates a death domain adapter in development. Nature 2001;414(6866):913-6.

Headon DJ, Overbeek PA. Involvement of a novel Tnf receptor homologue in hair follicle induction [see comments]. Nat Genet 1999;22(4):370-4.

Henke N, Schmidt-Ullrich R, Dechend R, Park JK, Qadri F, Wellner M, et al. Vascular endothelial cell-specific NF-kappaB suppression attenuates hypertension-induced renal damage. Circ Res 2007;101(3):268-76.

Horsley V, Aliprantis AO, Polak L, Glimcher LH, Fuchs E. NFATc1 balances quiescence and proliferation of skin stem cells. Cell 2008;132(2):299-310.

Hsu YC, Li L, Fuchs E. Transit-amplifying cells orchestrate stem cell activity and tissue regeneration. Cell 2014;157(4):935-49.

Kere J, Srivastava AK, Montonen O, Zonana J, Thomas N, Ferguson B, et al. X-linked anhidrotic (hypohidrotic) ectodermal dysplasia is caused by mutation in a novel transmembrane protein. Nat Genet 1996;13(4):409-16.

Krappmann D, Wulczyn FG, Scheidereit C. Different mechanisms control signal-induced degradation and basal turnover of the NF-kappaB inhibitor IkappaB alpha in vivo. Embo J 1996;15(23):6716-26.

Le Bail O, Schmidt-Ullrich R, Israel A. Promoter analysis of the gene encoding the I kappa B-alpha/MAD3 inhibitor of NF-kappa B: positive regulation by members of the rel/NF-kappa B family. Embo J 1993;12(13):5043-9.

Liu Y, Lyle S, Yang Z, Cotsarelis G. Keratin 15 promoter targets putative epithelial stem cells in the hair follicle bulge. J Invest Dermatol 2003;121(5):963-8.

Marko L, Vigolo E, Hinze C, Park JK, Roel G, Balogh A, et al. Tubular Epithelial NF-kappaB Activity Regulates Ischemic AKI. J Am Soc Nephrol 2016.

Mikkola ML, Pispa J, Pekkanen M, Paulin L, Nieminen P, Kere J, et al. Ectodysplasin, a protein required for epithelial morphogenesis, is a novel TNF homologue and promotes cell-matrix adhesion. Mech Dev 1999;88(2):133-46.

Momeni P, Glockner G, Schmidt O, von Holtum D, Albrecht B, Gillessen-Kaesbach G, et al. Mutations in a new gene, encoding a zinc-finger protein, cause tricho-rhino-phalangeal syndrome type I. Nat Genet 2000;24(1):71-4.
Mou C, Jackson B, Schneider P, Overbeek PA, Headon DJ. Generation of the primary hair follicle pattern. Proc Natl Acad Sci U S A 2006;103(24):9075-80. Epub 2006 Jun 12.
Mucenski ML, Wert SE, Nation JM, Loudy DE, Huelsken J, Birchmeier W, et al. beta-Catenin is required for specification of proximal/distal cell fate during lung morphogenesis. J Biol Chem 2003;278(41):40231-8.
Muller-Rover S, Handjiski B, van der Veen C, Eichmuller S, Foitzik K, McKay IA, et al. A comprehensive guide for the accurate classification of murine hair follicles in distinct hair cycle stages. J Invest Dermatol 2001;117(1):3-15.
Naito A, Yoshida H, Nishioka E, Satoh M, Azuma S, Yamamoto T, et al. TRAF6-deficient mice display hypohidrotic ectodermal dysplasia. Proc Natl Acad Sci U S A 2002;99(13):8766-71.
Nowak JA, Polak L, Pasolli HA, Fuchs E. Hair follicle stem cells are specified and function in early skin morphogenesis. Cell Stem Cell 2008;3(1):33-43.
Powolny-Budnicka I, Riemann M, Tanzer S, Schmid RM, Hehlgans T, Weih F. RelA and RelB transcription factors in distinct thymocyte populations control lymphotoxin-dependent interleukin-17 production in gammadelta T cells. Immunity 2011;34(3):364-74.
Pummila M, Fliniaux I, Jaatinen R, James MJ, Laurikkala J, Schneider P, et al. Ectodysplasin has a dual role in ectodermal organogenesis: inhibition of Bmp activity and induction of Shh expression. Development 2007;134(1):117-25.
Rhee H, Polak L, Fuchs E. Lhx2 maintains stem cell character in hair follicles. Science 2006;312(5782):1946-9.
Schmidt-Ullrich R, Aebischer T, Hulsken J, Birchmeier W, Klemm U, Scheidereit C. Requirement of NF-kappaB/Rel for the development of hair follicles and other epidermal appendices. Development 2001;128(19):3843-53.
Schmidt-Ullrich R, Memet S, Lilienbaum A, Feuillard J, Raphael M, Israel A. NF-kappaB activity in transgenic mice: developmental regulation and tissue specificity. Development 1996;122(7):2117-28.
Schmidt-Ullrich R, Paus R. Molecular principles of hair follicle induction and morphogenesis. Bioessays 2005;27(3):247-61.
Schmidt-Ullrich R, Tobin DJ, Lenhard D, Schneider P, Paus R, Scheidereit C. NF-kappaB transmits Eda A1/EdaR signalling to activate Shh and cyclin D1 expression, and controls post-initiation hair placode down growth. Development 2006;133(6):1045-57.
Sha WC, Liou HC, Tuomanen EI, Baltimore D. Targeted disruption of the p50 subunit of NF-kappa B leads to multifocal defects in immune responses. Cell 1995;80(2):321-30.
Shinkura R, Kitada K, Matsuda F, Tashiro K, Ikuta K, Suzuki M, et al. Alymphoplasia is caused by a point mutation in the mouse gene encoding Nf-kappa b-inducing kinase. Nat Genet 1999;22(1):74-7.
St-Jacques B, Dassule HR, Karavanova I, Botchkarev VA, Li J, Danielian PS, et al. Sonic hedgehog signaling is essential for hair development. Curr Biol 1998;8(19):1058-68.
Tomann P, Paus R, Millar SE, Scheidereit C, Schmidt-Ullrich R. Lhx2 is a direct NF-kappaB target gene that promotes primary hair follicle placode down-growth. Development 2016;143(9):1512-22.
Tornqvist G, Sandberg A, Hagglund AC, Carlsson L. Cyclic expression of lhx2 regulates hair formation. PLoS Genet 2010;6(4):e1000904.
Vidal VP, Chaboissier MC, Lutzkendorf S, Cotsarelis G, Mill P, Hui CC, et al. Sox9 is essential for outer root sheath differentiation and the formation of the hair stem cell compartment. Curr Biol 2005;15(15):1340-51.
Yan M, Zhang Z, Brady JR, Schilbach S, Fairbrother WJ, Dixit VM. Identification of a Novel Death Domain-Containing Adaptor Molecule for Ectodysplasin-A Receptor that Is Mutated in crinkled Mice. Curr Biol 2002;12(5):409-13.
Yilmaz ZB, Weih DS, Sivakumar V, Weih F. RelB is required for Peyer's patch development: differential

regulation of p52-RelB by lymphotoxin and TNF. EMBO J 2003;22(1):121-30.
Yin L, Wu L, Wesche H, Arthur CD, White JM, Goeddel DV, et al. Defective lymphotoxin-beta receptor-induced NF-kappaB transcriptional activity in NIK-deficient mice. Science 2001;291(5511):2162-5.
Yu HM, Jerchow B, Sheu TJ, Liu B, Costantini F, Puzas JE, et al. The role of Axin2 in calvarial morphogenesis and craniosynostosis. Development 2005;132(8):1995-2005.
Zhang B, Tsai PC, Gonzalez-Celeiro M, Chung O, Boumard B, Perdigoto CN, et al. Hair follicles' transit-amplifying cells govern concurrent dermal adipocyte production through Sonic Hedgehog. Genes Dev 2016;30(20):2325-38.
Zhang Y, Andl T, Yang SH, Teta M, Liu F, Seykora JT, et al. Activation of {beta}-catenin signaling programs embryonic epidermis to hair follicle fate. Development 2008;135(12):2161 - 72.
Zhang Y, Tomann P, Andl T, Gallant NM, Huelsken J, Jerchow B, et al. Reciprocal requirements for EDA/EDAR/NF-kappaB and Wnt/beta-catenin signaling pathways in hair follicle induction. Dev Cell 2009;17(1):49-61.